Avidity binding of human adenovirus serotypes 3 and 7 to the membrane cofactor CD46 triggers infection

Trinh, H V ; Lesage, G ; Chennamparampil, V ; Vollenweider, B ; Burckhardt, C J ; Schauer, S ; Havenga, M ; Greber, U F ; Hemmi, S

Abstract: The species B human adenoviruses (short Ad) infect cells upon attaching to CD46 or desmoglein-2 (DSG-2) by one or several of their twelve fiber knob trimers (FK). To test whether DSG-2 and CD46 simultaneously serve as virus receptors for Ad3, we performed individual and combined CD46/DSG-2 loss-of-function studies in human lung A549 and 16HBE14o cells. Our results suggest that in these cells, DSG-2 functions as major attachment receptor for Ad3, whereas CD46 exerts a minor contribution to virus attachment and uptake in the range of 10%. However, in other cells the role of CD46 may be more pronounced depending on, e.g., the expression levels of the receptors. To test if avidity allows Ad3/7 to use CD46 as receptor, we performed gain-of-function studies in rodent cells. The cell surface levels of ectopically expressed CD46 in CHO or human M010119 melanoma cells lacking DSG-2 positively correlated with Ad3/7 infections, while Ad11/35 infections depended on CD46 but less on CD46 levels. Antibody cross-linked soluble CD46 blocked Ad3/7/11/35 infections, while soluble CD46 alone blocked Ad11/35 but not Ad3/7. Soluble Ad3/7-FKs poorly inhibited Ad3/7 infection of CHO-CD46 cells, illustrating that Ad3/7-FKs bind with low affinity to CD46. This was confirmed by Biacore plasmon resonance studies. Ad3/7 FK binding to immobilized CD46 at low density was not detected, unlike Ad11/35-FK. At higher CD46 densities, however, Ad3/7-FK bound to CD46 with only 15-fold higher dissociation constants than Ad11/35-FK. These data show that an avidity mechanism for Ad3/7 binding to CD46 leads to infection of CD46-positive cells.

DOI: https://doi.org/10.1128/JVI.06181-11

Avidity binding of human adenovirus serotypes 3 and 7 to the membrane cofactor CD46 triggers infection

Hung V. Trinh[1,2†], Guillaume Lesage[1,2†], Venus Chennamparampil[1], Benedikt Vollenweider[1], Christoph J. Burckhardt[1‡], Stefan Schauer[3], Menzo Havenga[4§], Urs F. Greber[1] and Silvio Hemmi[1*]

[1]*Institute of Molecular Life Sciences, University of Zurich, Winterthurerstrasse 190, CH-8057 Zurich, Switzerland*

[2]*Life Science Zurich Graduate School, Molecular Life Science Program*

[3]*Functional Genomics Center Zurich, University of Zurich, Winterthurerstrasse 190, Zurich 8057, Switzerland*

[4]*Crucell Holland BV, Archimedesweg 4, 2333 CN Leiden, The Netherlands*

[†]Equal contribution

Corresponding author:* Dr. Silvio Hemmi, *Institute of Molecular Life Sciences Zurich, Winterthurerstrasse 190, CH-8057 Zurich, Switzerland; Phone: +41 44 635 3120; Fax: +41 44 635 6811; E-mail: silvio.hemmi@imls.uzh.ch*

[‡]*Present address: Department of Cell Biology, Harvard Medical School, Boston, Massachusetts 02115, USA*

[§]*Present address: Batavia Bioservices BV, Zernikedreef 9, 2333 CK Leiden, The Netherlands*

Abbreviations: Ad, adenovirus; CAR, Coxsackie virus B and Ad receptor; FK, fiber knob; MFI, mean fluorescence intensity; MOI, multiplicity of infection; MV, measles virus; p.i. post infection; ROI region of interest; RU, resonance units; SPR, surface plasma resonance; vp, virus particle

Running title: Species B adenovirus receptor

Abstract: 250 words
Total text including ref: 12,513 words

Abstract

The species B human adenoviruses (short Ad) infect cells upon attaching to CD46 or desmoglein-2 (DSG-2) by one or several of their twelve fiber knob trimers (FK). To test whether DSG-2 and CD46 simultaneously serve as virus receptors for Ad3, we performed individual and combined CD46/DSG-2 loss-of-function studies in human lung A549 and 16HBE14o cells. Our results suggest that in these cells, DSG-2 functions as major attachment receptor for Ad3, whereas CD46 exerts a minor contribution to virus attachment and uptake in the range of ~ 10%. However, in other cells the role of CD46 may be more pronounced depending on, e.g., the expression levels of the receptors. To test if avidity allows Ad3/7 to use CD46 as receptor, we performed gain-of-function studies in rodent cells. The cell surface levels of ectopically expressed CD46 in CHO or human M010119 melanoma cells lacking DSG-2 positively correlated with Ad3/7 infections, while Ad11/35 infections depended on CD46 but less on CD46 levels. Antibody cross-linked soluble CD46 blocked Ad3/7/11/35 infections, while soluble CD46 alone blocked Ad11/35 but not Ad3/7. Soluble Ad3/7-FKs poorly inhibited Ad3/7 infection of CHO-CD46 cells, illustrating that Ad3/7-FKs bind with low affinity to CD46. This was confirmed by Biacore plasmon resonance studies. Ad3/7 FK binding to immobilized CD46 at low density was not detected, unlike Ad11/35-FK. At higher CD46 densities, however, Ad3/7-FK bound to CD46 with only 15-fold higher dissociation constants than Ad11/35-FK. These data show that an avidity mechanism for Ad3/7 binding to CD46 leads to infection of CD46-positive cells.

Introduction

Human *Adenoviridae* comprise 55 types, classified into seven species, A to G (http://www.vmri.hu/~harrach/AdVtaxlong.htm), based on genome sequence comparison, hemagglutination and additional features. The B1 viruses Ad3, Ad7, Ad16, Ad21, Ad50 (short Ad3/7/16/21/50) predominantly infect the upper respiratory tract, whereas the B2 viruses Ad11/14/34/35 are associated with kidney and urinary tract infections with fatal outcome in immune-compromised patients (30, 54, 68). Recent epidemiological reports described the reemergence of several of these virus types associated with outbreaks of respiratory disease (7, 32, 39, 77). The tropism of species B viruses is broader than that of the C species, and includes cancer cells, dendritic cells and hematopoietic stem cells. This feature makes the B species interesting vectors for gene therapy and vaccination approaches (52).

Ads attach to their host cells by binding of the trimeric fiber protein to a cellular surface receptor. The fiber protein consists of a tail for anchorage to the penton base, a shaft of variable length, and a globular fiber knob (FK). The latter is responsible for the binding of the virus particle to a primary attachment receptor (43). Species B Ads bind different cell surface receptor(s) than most of the other species members (76). Two receptors have been identified, CD46 for Ad11 (57), Ad35 (15) and Ad3 (60), and species D Ad37 and Ad49 (31, 74), and desmoglein 2 (DSG-2) for Ad3/7/11/14 (69, 70). If CD46 functions as an attachment receptor for all species B types has been controversial. Virus competition, CD46 antibody blocking, and siRNA knock down of CD46 experiments suggested that more than one receptor exists for species B Ads (15, 19, 37, 56, 57, 60, 67). It was suggested that all species B Ads except Ad3/7 would utilize CD46, and all serotypes including Ad3/7 would bind to a second, common receptor (sBAR) (37, 56). Another group proposed an alternative classification, where group I members (Ad16/21/35/50) would almost exclusively use CD46, while group II members (Ad3/7/14) would not use CD46 but DSG-2, and the only member of group III (Ad11p) would be able to use both receptors (67, 70). Both classifications contrast, however, with findings by others, who reported functional utilization of CD46 by Ad3 and Ad7 in rodent cells ectopically expressing CD46 (13, 14, 20, 40, 60, 61).

Affinity analysis of monovalent interactions of different species B FKs to CD46 SCR I-II revealed a broad range of affinities, with similar dissociation constants (K_D) for Ad11 and Ad35-FK (Ad11/35-FK) in the range of 5 to 19 nM, but strongly increased K_D values of 284 nM for Ad21-FK and 437 nM for Ad16-FK, and an about 2,000-fold reduced affinity for both, Ad7-FK and Ad14-FK to CD46 SCR I-II, compared to Ad11-FK (10, 47, 48). The crystal structures of FKs for Ad3 (11), Ad35 (46, 71), Ad16 (47), and Ad7/14 (48) have revealed a generally conserved overall fold and trimeric organization. Interestingly, the different FKs have low sequence identity, especially at the surface loops, which mediate binding to CD46, as indicated by co-crystal structures of CD46 SCR I-II with Ad11-FK (49), or Ad21-FK (10). These crystal structures also suggested interactions of the trimeric fiber molecule with three CD46 molecules, albeit involving substantial differences in the number and types of contacts. The binding surface on CD46 SCR I-II for Ad11-FK comprises a large continuous area of 1,681 $Å^2$, with three main contact points composed of fiber knob DG, HI and the IJ loop residues. A more recent co-crystal structure of Ad11-FK in complex with an extended CD46 SCR I-IV confirmed the involvement of the DG and HI loops, but not of the IJ loop (50). Together, this wealth of structural evidence indicates that there are no central binding motifs among species B Ads, which would explain the macroscopic observations that there is a wide range of affinities for CD46 between the different FKs (10, 47, 71).

Here we tested two hypotheses, first that DSG-2 and CD46 simultaneously serve as receptors for Ad3, and second, that avidity effects allow the low affinity CD46-binders Ad3/7-FK to attach to CD46, and thereby grant these viruses to use CD46 as an entry receptor. We performed loss-of-function studies in human A549 and 16HBE14o lung cells and showed that DSG-2 functions as a major attachment receptor for Ad3, whereas CD46 exerts a minor contribution in the range of ~ 10% to virus attachment and up-take. Gain-of-function in CD46-negative CHO or CD46-low human melanoma cells both negative for DSG-2 demonstrated that Ad3/7 infections increased with increasing levels of ectopic CD46. We further showed that multimerized soluble CD46 blocked Ad3/7 infections, and that Ad3/7-FK reduced Ad3/7 infections in A549 cells expressing high levels of CD46. Finally, biosensor

measurements demonstrated that affinities of Ad3/7-FKs to immobilized CD46 increased at high receptor densities. These data argue that CD46 is a receptor for all species B adenoviruses if present at sufficient levels, and may function together with or separately from DSG-2.

Materials and Methods

Viruses and cells.

Ad3CMV-eGFP, Ad7CMV-eGFP Ad11CMV-eGFP and Ad35CMV-eGPF containing the CMV-eGFP expression cassette in the deleted E1 region were prepared at concentrations of $7.1x10^{11}$, $1.6x10^{11}$, $6.6x10^{11}$ $1.3x10^{12}$ virus particles (vp)/ml and have been described previously (13, 14). Ad3 (prototype strain GB), Ad7 (prototype strain Gomen), Ad11p and Ad35 (Holden strain) were radio labeled as described (14). Specific activities were in the range of 2.6×10^{-5} to 4.9×10^{-5} cpm/vp. Likewise, Ad2, Ad3 and Ad35 were labeled with atto488 (Atto-tec, Germany) similar as described (65).

Chinese hamster cell lines CHO-K1 and CHO-15B6 (containing a mutation in the N-acetylglucosamininyl-transferase 1), the human 293T and 911 embryonic kidney cells, and the A549 lung carcinoma cells were grown in Dulbecco's modified Eagle's medium (DMEM) plus 8% fetal bovine serum (FBS). The human 16HBE14o bronchial epithelial cells (17) and the primary human melanoma cell cultures M010119 (55) were grown in RPMI 1640 plus 8% FBS as described earlier. CHO-CD46 cell lines stably expressing the BC1 splice isoform were generated as described for the BHK-CD46 cells (60). For stable transfection of CHO-15B6 and M010119 cells with the N-terminal eGFP-tagged CD46-encoding cDNA (eGFP-CD46), a PCR-amplified CD46 sequence was cloned into pcDNA3.1-CARSP-eGFP-CAR (5), replacing the mature Coxsackie virus B and Ad receptor (CAR) cDNA. In the resulting construct, the 19 amino acid residues of the human CAR signal peptide sequence were followed by two spacer residues, 239 residues of eGFP, ten additional spacer residues, and 344 residues of the mature CD46 BC1 isoform. To avoid eGFP-induced dimerization of the tagged CD46, an A206K mutant of eGFP was utilized (75). Following selection in DMEM plus 8% FBS and 0.8 mg/ml G418, individual clones were picked and screened giving rise to the limiting dilution clone CHO-eGFP-CD46#33.5. To generate human melanoma M010119 and lung carcinoma A549 cells expressing eGFP-CD46, a lentiviral expression system was used. For this, the eGFP-CD46 cDNA was subcloned into the lentiviral pBlasti vector (27), and lentiviral vectors were generated by transient transfection in 293T cells.

M010119 and A549 cells transduced with lentiviral vector pBlasti-eGFP-CD46 were selected in blasticidin-containing medium at 4 µg / ml. Resulting bulk cultures M010119-eGFP-CD46#8 and A549-eGFP-CD46#2 revealed homogenous CD46 expression.

Immune reagents.

Cytofluorometric analysis, CD46-specific antibodies and secondary fluorochrome conjugates have been described previously (14, 60). The hybridoma cell line secreting the MCI20.6 anti-CD46 antibody was a generous gift from Denis Gerlier (42). Monoclonal 8E5- and 6D8-anti desmoglein 2 were purchased from Santa Cruz Inc., and goat anti-human IgG-Fc from BETHYL Laboratories Inc..

Virus binding and transduction assays.

Binding experiments including radio-labeled Ads were performed as described previously (14). For binding experiments using atto488-labeled viruses, the same procedure was used, except cells were analyzed by cytofluorometric means. For eGFP expression analysis, triplicates of 10^5 cells were seeded in 12-well plates. After incubation for 3 h at 37°C, 5% CO_2, the cells were infected with recombinant eGFP-expressing Ads at virus concentrations of 10, 100, or 1,000 vp/cell. Medium was replaced 5 h p.i., and cells were analyzed two days p.i. by flow cytometric analysis (Cytomics FC 500; Beckman Coulter).

For FK competition experiments, cells were seeded in triplicate 12-well plates and were allowed to adhere as above. After 3 h, the medium was removed and the cells were washed with cold PBS. For blocking with FK proteins, serial 5-fold dilutions of the different FKs were prepared in PBS, resulting in concentrations of 5,000, 1,000, 200, 40, and 8 ng/ml. 500 µl of FK dilutions were added to the cells and incubated for 1 h on ice under constant shaking. Subsequently, eGFP-encoding Ad vectors were added and incubated for 1 h. The amount of virus added was optimized in preceding experiments and was adjusted such that for all five eGFP-expressing

vectors, similar reporter expression levels in the range of 100 to 500 were obtained by FACS measurement. Thus, for A549 cell transduction, Ad3-, 5-, 7-, 11-, and 35-eGFP vectors were used at 14,800, 2,825, 8,200, 1,314 and 2,540 vp/cell, respectively. For CHO-CD46#2, the virus input was adjusted to 29,600, 2,825, 8,200, 657 and 1,088 vp/cell, respectively. The cells were washed twice with cold PBS and were returned to standard cell culture conditions. Analysis of cells was performed two days p.i., as described above. For competition experiments including recombinant CD46ex-huFc, FK proteins were replaced with the indicated concentrations of CD46ex-huFc or CARex-huFc. In case of including cross-linking of CD46ex-huFc and CARex-huFc, the adapter proteins were pre-incubated on ice with goat anti-human IgG antibody for 30 min before adding to the cells. Specific siRNAs for CD46 (15) and DSG-2 (70) were synthesized by Microsynth (Switzerlandand) and scrambled siRNA control was obtained from Qiagen. siRNA transfections were performed with Lipofectamine 2000 (Invitrogen) for A549 cells and Interferin (Polyplus) for 16HBE14o cells. Knock down cells were infected with recombinant eGFP-expressing Ads at virus concentrations of 500 vp/cell. Statistical evaluation was performed using Student's *t* test.

Generation of recombinant soluble Ad receptor and fiber knob proteins. Production of the soluble CD46ex-huFc and CARex-huFc has been described earlier (12, 60). CD46ex-huFc comprises 295 amino acids of the mature extracellular domain including all SCR I-IV domains, the STP of BC1, plus the short region of unknown function, fused to the 232 amino acids of the human IgG1-Fc domain including hinge, CH2 and CH3 regions. Production of CD46-SCR I-II consisting of 145 amino acids, including a N-terminal his-tag and spacer, has been described in (14). CARex-huFc protein comprises the extracellular domain of CAR fused to the human IgG1-Fc domain. The five recombinant FKs derived from Ad3, 5, 7, 11, and 35 were produced using the Bac-to-Bac baculovirus expression system (pFastBac, Stratagene). All FKs contained a N-terminal 6xhis-tag used for single step Ni-NTA-agarose affinity chromatography, followed by the recognition site for TEV protease. FK comprised the fiber sequence residues 114 to 319 for Ad3 (NCBI gene bank ID

(GI) 78059423), 384 to 581 for Ad5 (GI: 56160559), 126 to 325 for Ad7 (GI: 51173336), 126 to 325 for Ad11 (GI: 56160807), and 126 to 323 for Ad35 (GI: 56160945). Calculated weights of the FK monomer/trimers were 26.28/78.85, 24.98/74.95, 25.63/76.89, 25.90/77.71, and 25.50/76.50 kDa for FK of Ad3, 5, 7, 11, and 35, respectively.

Surface plasmon resonance analysis for kinetics/affinity between CD46 and Ad-FKs

Surface plasmon resonance (SPR) experiments were performed on a Biacore T100 system (GE Healthcare) at 25°C equipped with CM5 sensor chips. All reagents including amine-coupling kit, HBS-P+ and CM5 chips were purchased from Biacore (GE Healthcare). Buffer HBS-P+ pH 7.4 (10 mM HEPES, pH 7.4, 150 mM NaCl, 0.05% (v/v) Surfactant P20) was used as running buffer for the entire measurement. Each CM5 chip contained four flow cells, designated Fc1-Fc4. The Fc2/Fc4 were used to immobilize the CD46ex-huFc ligand, while Fc1/Fc3 were used to immobilize the CARex-huFc ligand. The immobilization procedure included three steps; surface activation by using a 1:1 mix of 0.4 M 1-ethyl-3-(3-dimethylaminopropyl)-carbodiimide in water (EDC) and 0.1 M N-hydroxysuccinimide in water (NHS) for 420 s with a flow rate of 5 µl/min, immobilization of 0.12 µM ligands in 10 mM sodium acetate pH 4.0 buffer, and deactivation of excess reactive groups by using 1 M ethanolamine-HCl pH 8.0 for 420 s with a flow rate of 5 µl/min. Following completion of immobilization, the sensor chip was conditioned three times with 50 mM NaOH to stabilize the surface. For initial binding assays, Ad3-, 11- and 35-FK analytes were injected at 18.75 and 150 nM, and Ad7-FK at 11.07 and 88.59 nM in HBS-P+ buffer at either 30 or 50 µl/min using a contact time of 240 or 280 s. For kinetic studies, Ad3, 7, 11 and 35 FK analytes were injected at 0.27, 0.82, 2.47, 7.41, 22.22 and 66.67 nM in HBS-P+ buffer at either 30 or 50 µl/min using a contact time of 300 or 360 s and a dissociation time of 3,600 s. After each binding cycle, the CM5 surface chip was regenerated by injection of 3 M $MgCl_2$ for 30 to 45 s, followed NaOH in a range of 4–50 mM for 20 s. All analyte concentrations were repeated twice and the obtained sensograms were corrected by subtracting the data from the reference flow cell and

240 from blank buffer injections (double referencing). For details of kinetic and affinity
241 analysis as well as fitting procedure see supplemental Methods.

242

Results

CD46 and Desmoglein 2 simultaneously serve as Ad3 receptor.

To test whether CD46 and DSG-2 simultaneously or additively serve as attachment receptors, we performed loss-of-function studies in human lung carcinoma A549 cells. These cells stained positive for CD46 (sFig. 1A) and DSG-2 (sFig. 1B) expression, revealing arbitrary mean fluorescence intensities (MFI) of 74 and 29, respectively. We tested antibodies against CD46, DSG-2 and a mix of both, and determined their effects on Ad3 and Ad35 binding. For this, cells were incubated with 1,000 vp of atto488-labeled wild type Ad3/35 followed by determination of cell-associated viruses by cyto-fluorometric analysis. When compared to PBS and anti-CAR antibody controls, pre-incubation of A549 cells with the known CD46 blocking antibody MEM258 (14) gave 13 and 8% reduction of Ad3 binding at the highest concentration of 20 µg/ml, respectively (Fig. 1A). This is in agreement with earlier results reporting inhibition of Ad3 binding to human cells, for example, 40% binding reduction to human K562 cells (60), or up to 48% inhibition for human hepatoblastoma HuH-7 cells (67). Pre-incubation with increasing concentrations of DSG-2 antibodies on the other side resulted in 47 and 42% reduction of Ad3 binding at 4 and 40 µg/ml, respectively, which is comparable to the approximately 60% maximal inhibition reported by Wang *et al.* using twice the concentration of the same mix of antibodies used here (70). Interestingly, when CD46 and DSG-2-specific antibodies were combined, we noticed a significant additive inhibition resulting in 70% inhibition of Ad3 binding. In comparison, the high concentrations of CD46 antibody reduced Ad35 binding by 93 and 98%, but the DSG-2 antibody mix had no significant effects (Fig. 1B). These results are consistent with the notion that Ad35 uses CD46 but not DSG-2 as an attachment receptor (13, 67).

We next performed siRNA-mediated knock down of CD46, DSG-2 and both receptors together, and analyzed these cells for virus binding and transduction. Initial tests for optimizing siRNA concentrations confirmed that best CD46 down-regulation was obtained using a single CD46-specific siRNA at 5 nM, whereas a pool

of four DSG-2-specific siRNAs each at 5 nM was optimal for DSG-2 protein downregualtion when measured by cytofluorometric analyses (15, 70). In five independent experiments, siRNA-mediated reduction of CD46 was in the range of 74 to 88% with a mean of 82%, when using the CD46-specific siRNA alone, and 67 to 86% with a mean of 77%, when using the CD46-specific siRNA in combination with DSG-2-specific siRNAs (see Fig. 1C for a representative experiment). Similarly, siRNA-mediated reduction of DSG-2 was in the range of 68 to 80% with a mean of 73%, when using the DSG-2 siRNAs alone, and 63 to 82% with a mean of 71%, when using the DSG-2 siRNAs in combination with the CD46 siRNA. When binding of atto-488 labeled Ad3 to these cells was analyzed, we noticed that in CD46 siRNA-only-cells binding was reduced by 28% in the experiment shown in Fig. 1D, whereas binding of Ad3 to DSG-2 siRNA-only-cells was reduced by 66%. Similar as for the antibody blocking experiments, combination of both siRNAs additively reduced Ad3 binding to 77%. Of note, the additive Ad3 binding reduction was not paralleled by a reduction of the DSG-2 expression level in the siRNA combination cells, indicating specificity for CD46. The range of reduction varied from 3 to 23%, with a mean of 11%. As for the antibody inhibition experiment, Ad35 attachment was mainly affected by CD46 but not DSG-2 interference, resulting in 76 and 77% binding reduction for CD46-only siRNA and CD46 plus DSG-2 siRNAs, respectively. Attachment of the CAR-binding Ad2 was not affected in these cells, demonstrating the specificity of the observed virus binding reduction for Ad3/35.

We then used the four different siRNA cells to analyze transduction by Ad5, Ad3 and Ad35-eGFP reporter viruses. CD46 interference gave no decrease in eGFP expression for Ad3/5 (Fig. 1E). However, Ad3-eGFP-mediated expression was reduced by 71% in DSG-2 siRNA-treated cells and by 82% in DSG-2 plus CD46 siRNA combination cells, revealing a small additive effect of 11% (Fig. 1E). The additive reduction in Ad3 infection by siRNA combination cells was reproducibly significant, and varied from 11 to 17%, with a mean of 13% in 4 of 5 experiments. It should be noted here that CD46 down-regulation had a very small effect on the transduction by Ad35-eGFP. We therefore repeated this experiment using a chimeric Ad5 containing the fiber knob and shaft from Ad35 (Ad5-eGFP-FK35), and found a

60% reduction of transgene expression upon CD46 siRNA silencing (data not shown). This was similar to data from others using a similar fiber chimeric vector (15). As suggested earlier, a possible explanation for these observations includes that fiber-knob swapped vectors have altered intracellular trafficking or stability (63).

Using the same approach, we also tested human 16HBE14o bronchial epithelial cells, which are a commonly used model for respiratory epithelial cell infections (17, 35). These cells revealed about 2-fold lower CD46 (sFig. 1C) and 3-4-fold lower DSG-2 (sFig. 1D) expression, when compared to A549 cells. siRNA-mediated reduction of CD46 and DSG-2 was in average 89 and 91%, respectively, when using the single-specific siRNA alone or in combination (Fig. 1F). Binding of atto-488 labeled Ad3 in CD46 was reduced by 20 and 85% in CD46 and DSG-2 siRNA-only-cells, respectively, and combination of both siRNAs additively reduced Ad3 binding to 95% (Fig. 1G). When using the four different siRNAs cells to analyze transduction by eGFP reporter viruses, Ad3-eGFP-mediated expression was reduced by 48% in DSG-2 siRNA-treated cells and by 76% in DSG-2 plus CD46 siRNA combination cells, revealing an additive effect of 28% (Fig. 1H).

Taken together, our results suggest that A549 and 16HBE14o cells expressing both DSG-2 and CD46, DSG-2 functions as major attachment receptor for Ad3, whereas CD46 exerts an accessory role for binding and uptake. In other human cells, however, the CD46 contribution may be more pronounced depending, e.g., on the expression levels of the receptors.

Increasing ectopic expression of CD46 leads to enhanced transduction of Ad3/7/11/35 in rodent and human cells.

Avidity effects allow viruses to infect susceptible cells despite somewhat low affinity to cell surface receptors (22, 73). We therefore tested if avidity effects occur during interaction of the Ad3/7 serotypes in CD46-gain of function experiments. We and others had shown earlier that rodent cells such as hamster BHK and CHO cells, or mouse Ltk^- and B16 cells stably expressing CD46 become sensitive to infection with various species B human Ads, including Ad3/7/11/35 (13, 14, 20, 40, 60, 61).

To address if CD46 needs to be expressed at a certain threshold level to be an Ad3/7 receptor, we generated clonal CHO cells stably expressing different levels of the CD46 BC1 isoform and compared their binding and transduction for species B serotypes. Of note, rodent cells including unmodified CHO were found negative for Ad3 binding (15, 20, 37, 67, 70 and Fig. 2B)) and they did not stain with a DSG-2 antibody (data not shown), suggesting that they lack expression of DSG-2 or that hamster DSG-2 is not able to bind human Ad3. The highest levels of CD46 were measured in CHO-CD46#2 cells with an arbitrary mean fluorescence intensity (MFI) of 161, followed by CHO-CD46#1 (MFI of 45), and CHO-CD46#6 (MFI of 33) (sFig. 1A). All three CHO clones were derived from CHO-15B6 cells. Additional CHO-CD46#RC cells, which were derived from CHO-K1 cells (4) and expressed similar CD46 levels as CHO-CD46#1 were included as controls in the transduction study. These cells gave similar data to CHO-CD46#1 and are not shown here. We noticed, however, that the CD46 stably transfected cells had broader expression ranges than for example human lung carcinoma A549 cells, which had an MFI of 74. We therefore used the stable CD46 expressing CHO cells at low passage numbers to ensure comparable expression levels. Cells were incubated with 1,000 vp of [^{3}H]-thymidine-labeled wild type Ad3/7/11/35 followed by determination of cell-associated viruses by liquid scintillation counting (Fig. 2A). CHO-CD46#2 cells expressing the highest levels of CD46 revealed highest virus binding for all four viruses, followed by CHO-CD46#1 and CHO-CD46#6 cells, which bound 2-4-fold more virus compared to parental CHO cells. Binding of Ad3/7/11 to A549 cells was intermediate compared to CHO-CD46#2 and CHO-CD46#1 cells, whereas binding of Ad35 was higher to A549 than CHO-CD46#2 cells.

Since binding experiments have a relatively low dynamic range, we performed transduction experiments using eGFP-expressing vectors. Increasing amounts of recombinant Ad3/7/11/35 expressing eGFP gave a robust increase of transgene expression in all four CHO-CD46 cells (including CHO-CD46#RC cells) (Fig. 2B and Table 1). At a virus concentration of 1,000 vp/cell, e.g., Ad3-mediated eGFP expression increased 18-fold in CHO-CD46#6 cells, 55-fold in CHO-CD46#1 cells, and 192-fold in CHO-CD46#2 cells, when compared to parental CHO cells. When

standardized to A549 cells, Ad3-eGFP-mediated transgene expression levels amounted to 0.24% in parental CHO cells, 19% in CHO-CD46#6 cells (with 2.2-fold lower CD46 than A549), 60% in CHO-CD46#1 cells (with about 1.5-fold lower CD46 than A549), and 211% in CHO-CD46#2 cells (2.2-fold higher CD46 than A549). For better comparison of transduction efficiency, vp/cell concentrations necessary to reach the arbitrary MFI value of 100 were calculated (Table 1). These values showed that highest input of 8,207 Ad3 vp/cell was needed for CHO-CD46#6 cells, 2,597 vp/cell for CHO-CD46#1 cells, and 717 vp/cell for CHO-CD46#2 cells to reach comparable transduction levels. Transduction with Ad7 was about 2-fold more efficient than Ad3 when comparing vp/ml values necessary to reach MFI of 100. Ad11/35 consistently transduced all tested cells more efficiently than Ad3/7, including control A549 cells and parental CHO cells. When standardized to Ad35, Ad3 infection of CHO-CD46#6, #1, #2 and A549 required 27, 16, 4.2 and 2.7-fold higher vp input to obtain the MFI value of 100, respectively. For Ad7, these numbers amounted to 9.5, 7.3, 1.57 and 1.1-fold. In contrast, Ad11 had a similar transduction efficacy as Ad35. Of note, when using Ad5-eGFP in these cells, transduction levels were within a factor of 2 for the different CD46-expressing clones including the parental CHO cells.

We also tested whether human melanoma M010119 cells with low CD46 expression (MFI of 17.8) (sFig. 1E) were increasingly transduced with Ad-eGFP vectors by increasing CD46 levels. Stable transfection of these cells (M010119-eGFP-CD46#8) resulted in about 9-fold higher CD46 expression levels (MFI of 155), compared to the parental cells. In this case, an N-terminal eGFP-tagged CD46 BC1 isoform was used, where the endogenous signal peptide was replaced by the CAR signal peptide, followed by the eGFP sequence and the sequence of the mature CD46 BC1 isoform. Of note, the receptor function of the eGFP-tagged CD46 form was retained for all four species B serotypes tested in M010119-eGFP-CD46#8 cells (Fig. 2C, Table 2). When using 1,000 vp/cell, M010119-eGFP-CD46#8 cells with the 9-fold higher CD46 level revealed 86, 26, 2.1 and 2.3-fold enhancements of reporter eGFP for Ad3/7/11/35 mediated transduction, respectively, when compared to parental M010119 cells. Determination of vp/cell ratios necessary to reach MFI value of 100,

revealed 127, 52, 3.1, and 2-fold enhancement of Ad3/7/11/35-mediated transduction, respectively. Of note, both, the parental M010119 low-CD46 cells as well as the M010119-eGFP-CD46#8 high-CD46 cells expressed no DSG-2, when analyzed by cytofluorometric means (sFig. 1B, F), in contrast to A549 cells, which expressed high levels of DSG-2.

In summary, ectopic expression of CD46 in rodent cells, or enhanced expression of CD46 in human cells low in CD46 and negative for DSG-2 resulted in increased transduction with Ad3/7/11/35 species B serotypes. Transduction efficacy of Ad3/7 correlated with CD46 density levels in these cells, whereas Ad11 reached a plateau with the medium CHO-CD46#1 cells and Ad35 was largely independent of the CD46 levels. This is compatible with the notion that Ad3/7 exhibit a lower affinity for CD46 than Ad11/35, but can compensate the lower affinity by avidity binding.

Cross-linking of soluble CD46 enhances blocking of Ad3 and Ad7 infection of CHO-CD46 and A549 cells.

We earlier documented that soluble CD46ex-huFc was at least 100-fold more potent at blocking Ad11/35 binding to rodent cells expressing CD46, when compared to Ad3 and 7 (13). To further test the hypothesis that avidity allows Ad3/7 to use CD46 as a functional receptor, we repeated the virus blocking assays with CD46ex-huFc, but included this time cross-linked adapter proteins. We reasoned that antibody-mediated cross-linking of CD46ex-huFc could provide locally more binding sites per molecule, mimicking the situation on the cell membrane where CD46 can diffuse freely and form clusters following multivalent binding (1, 9).

When using 50, 500, and 5,000 ng/ml of CD46ex-huFc protein alone, only Ad11-eGFP or Ad35-eGFP mediated transgene expression were significantly reduced in CHO-CD46#2 or A549 cells (Fig. 3A, B). In contrast, CD46ex-huFc did not result in significant reduction of Ad3/7 mediated transgene expression (sFig. 2A, B). However, when we combined CD46ex-huFc protein at a concentration of 500 ng/ml with 2-fold increasing amounts of cross-linking goat-anti human Fc antibody, significant blocking was also achieved for both Ad3 and Ad7-mediated transgene

426 expression. Inhibition followed a precipitin-type curve reaching a plateau in the range
427 of 500, 1,000 or 2,000 ng/ml of goat anti-human Fc. Highest blocking for Ad3-eGFP
428 amounted to 65% in CHO-CD46#2 cells and 83% in A549 cells, and for Ad7-eGFP,
429 the highest blocking was 77% in both cell types. We conclude that CD46ex-huFc
430 multimerization leads to efficient blocking of Ad3/7. A similarly multimerized complex
431 consisting of CARex-huFc had no significant effects on Ad3/7 infection, but CARex-
432 huFc inhibited Ad2/5 transduction (12, 38).

433

434 **Species B adenovirus fiber knobs cross-compete for CHO-CD46 and A549**
435 **transductions**

436 To further characterize affinity differences and receptor usage by species B Ads, we
437 performed blocking studies with species B Ads and soluble FKs in CHO-CD46#2 and
438 A549 cells. CHO-CD46#2 cells do not express DSG-2, unlike human A549 cells.
439 Virus inhibition assays were performed using five different eGFP-expressing vectors
440 as readout for binding and infectivity. For CHO-CD46#2 cells, Ad3/7/11/35-eGFP
441 inputs of 29,600, 8,200, 657, and 1,088 vp/cell, respectively, were used. For A549
442 cells, the virus inputs amounted to 14,800, 8,200, 1,314 and 2,540 vp/cell, and in
443 addition, for Ad5-eGFP an input of 2,825 was applied. The virus input concentrations
444 were chosen such that the unblocked transgene expression values amounted to
445 fluorescence intensities in the range of about 200, thereby allowing an optimal
446 dynamic range (not shown). We assured that FKs of Ad3/7/11/35 were
447 predominantly present in trimeric form (sFig. 3A, B). All five Ad FK proteins were
448 tested in a dose-dependent manner with the highest concentration of 5,000 ng/ml
449 diluted in a 5-fold dilution series to the lowest concentration of 8 ng/ml (Fig 4A, B and
450 Table 3). Specificity of this assay was confirmed by the finding that the species C
451 Ad5-FK only gave rise to inhibition of Ad5, but not for any of the species B serotypes.
452 Likewise, species B FKs only inhibited species B serotypes, but not Ad5-eGFP.

453 The cross-competition assays revealed differences in the capacity of the individual
454 FKs to compete with species B viruses. The Ad3/7-FKs on one side, and Ad11/35-
455 FKs on the other side showed similar behavior, which, however, was different in the

two cell types tested. In CHO-CD46#2 cells, Ad3/7-FKs elicited at best weak competition for corresponding and non-corresponding Ad3 and Ad7, and no effect on non-corresponding Ad11 and Ad35. This is illustrated by the 40% inhibition of Ad3-eGFP transduction at the highest Ad3-FK concentration of 5,000 ng/ml, and a non-significant 7% inhibition for Ad7-eGFP transduction. Ad3-FK concentrations necessary for 50% inhibition (FK-50%) were larger than the highest concentration available, and could thus not be calculated. Ad7-FK was more efficient than Ad3-FK, and using 5,000 ng/ml, 86 and 81% of Ad3/7-mediated eGFP expression was inhibited, respectively. FK-50% inhibition values for Ad7-FK were determined to be 169 and 2,690 ng/ml for Ad3/7-mediated transgene expression, respectively. In contrast, Ad11/35-FKs led to efficient blocking of all B-type viruses in these cells. Likewise, Ad35-FK blocking efficiency was in the range of 85 to 97% at 5,000 ng/ml, and the corresponding FK-50% values were 5, 63, 14 and 26 ng/ml.

The binding inhibition pattern for A549 cells was different than for CHO-CD46#2 cells. In A549 cells, Ad3/7-FKs efficiently competed for corresponding and non-corresponding Ad3/7 in A549 cells with FK-50% inhibition values of 25 and 23 ng/ml, respectively (Fig. 4B, Table 3). With highest concentrations of Ad7-FK, blocking efficiency of 95 and 87% was obtained for Ad3/7-mediated eGFP expression, respectively, with FK-50% values of 17 and 31 ng/ml, respectively. However, as for CHO-CD46#2 cells, Ad3/7-FKs revealed no effect on non-corresponding Ad11/35 in A549 cells. Ad11-FK efficiently blocked all four species B serotypes, with FK-50% inhibition values of 31, 87, 13, 13 ng/ml, whereas Ad35-FK was less efficient at inhibiting Ad3 and 7, with FK-50% values of 470, and 4’459 ng/ml, respectively, but very efficient at inhibiting Ad11 and 35, with FK-50% values of 33 and 5 ng/ml, respectively.

In summary, blocking studies with Ad3/7-FKs revealed different effects for corresponding viruses in CHO-CD46 cells or human A549 cells. In CHO-CD46 cells, the observed low blocking efficiency confirms the low affinity of the Ad3/7 soluble FK molecules to CD46. In contrast, the efficient blocking activity of Ad3/7-FK in A549 is compatible with our findings that up to 90% of Ad3 binds with a presumable higher affinity to DSG-2, whereas a minor fraction binds to CD46.

Binding and affinity determinations of CD46 to Ad3/7/11/35-FK by surface plasmon resonance.

To further characterize species B Ad interactions with CD46 we applied biosensor technology using soluble CD46 and the FKs of Ad3/7/11/35, which were predominantly present in trimeric form (sFig. 3A, B). Initial Biacore experiments using sensor chips had previously been described for immobilized FKs and monovalent CD46-SCR I-II as soluble analyte thereby avoiding avidity effects of CD46 (10, 47, 48, 71, 72). The SCR I-II domain comprised the binding sites for the FKs (14, 49, 53, 71). Under these conditions, we determined the affinities of Ad11/35-FK to CD46-SCR I-II, and found that they were consistent with a 1:1 (monophasic) binding model, where one surface FK monomer interacted with one soluble CD46-SCR I-II (data not shown). Ad3/7-FK, however, did not bind to immobilized CD46-SCR I-II, most likely due to low affinity of their monomers to CD46-SCRI-II, in agreement with earlier data for Ad7-FK (48).

In a reversed set-up of the SPR measurements we immobilized the extracellular domain of CD46 fused to human Fc (CD46ex-huFc, see 60) to the flexible dextran matrix of the sensor chip and used FKs as analytes. CD46ex-huFc is a disulfide-linked dimer, as suggested by native gel electrophoresis (sFig. 3C, and not shown). We first tested if different concentrations of immobilized CD46ex-huFc would give different binding responses for the FKs. Hereto, flow cell 2 (Fc2) of the CM5 sensor chip was coated with high density of CD46ex-huFc (2,630 resonance units, RU), and the control Fc1 with high density of CARex-huFc (3,431 RU). In a parallel set up, Fc4 was coated with low surface density of CD46ex-huFc (345 RU), and Fc3 with low density of CARex-huFc (278 RU). From the sensograms of Ad3/7/11/35-FK binding to CD46ex-huFc we noticed that higher concentrations of soluble Ad3/7-FK (150 and 89 nM, respectively) were required to reach equilibrium binding at high CD46ex-huFc density levels compared to Ad11/35-FK (18.75 nM) (Fig. 5A-D). At equilibrium binding, both Ad3/7-FK and Ad11/35-FK slowly dissociated, indicative of stable complexes. At low CD46ex-huFc density, the Ad11/35-FKs and to a very low extent also Ad7-FK but not Ad3-FK showed detectable binding. The absolute binding

values R_{max} varied by factors of 2-3 between Ad3 and Ad7-FK, and Ad11 and Ad35-FK, as well as different technical replicas of the experiments, possibly reflecting different degrees of FK purities and chip conditions.

Combined binding kinetics and affinity measurements were carried out for each of the four FKs. For this, we used three independent measurements in the range of 0.27, 0.82, 2.47, 7.41, 22.22 and 66.67 nM, and two different high-density CD46 biosensor chips of 2,630 RU and 1,121 RU. Both biosensor chips gave similar results (Fig. 5E-H, sTable 1). In addition, Ad3-FK binding was found to be independent of the flow rate at the standard flow rate of 30 µl/min and an increased flow rate of 55 µl/min, excluding the possibility that the binding reactions were influenced by mass transfer effects (41). The values for the kinetic rate constants were highly reproducible for the individual FKs, with low standard errors for the association and dissociation constants (see Fig. 5E-H, sTable 1). The kinetics and binding data could be best fitted to a two-stage reaction model rather than monophasic, or trivalent binding models (see equations in *supplemental Methods*). Modeling of the measured association and dissociation rate constants and R values was carried out based on global fittings for k_{a1}, k_{a2}, k_{d1} and k_{d2}, and local calculations of R_{max}, and % χ^2/R_{max}. All % χ^2/R_{max} values were below 5%. The average apparent K_D values (Table 4) were not significantly different for Ad3-FK (2.48 $x10^{-10}$ M) and Ad7-FK (3.70 $x10^{-10}$ M), whereas the apparent K_D for Ad11-FK and Ad35-FK were 10-15-fold lower (*P*=0.002/0.0669 for Ad3/7 compared to Ad11, and *P*=0.0014/0.063 for Ad3/7 *versus* Ad35) and amounted to 2.46 $x10^{-11}$ and 1.78 $x10^{-11}$ M, respectively. Thus, the 10-15-fold difference between the apparent K_D values for Ad3/7 and Ad11/35 at high CD46 densities deviated considerably from the 2,000-fold differences of K_D reported for the monovalent CD46 binding to Ad7-FK and Ad11-FK (48). Since the measurements were performed using similar set ups, this suggests that at high surface densities of CD46, trimeric FK interacts with two or even three CD46 binding sites and the resulting avidity effects overcome low affinity restrictions of single FK–CD46 interactions.

Discussion

The data obtained in this study suggest that both, DSG-2 and CD46 can serve simultaneously as Ad3 receptors and that avidity effects allow the low affinity CD46-binders Ad3/7-FK to attach to CD46 for infectious entry. Conspicuously, several Ad serotypes have been reported to utilize more than one attachment receptor, which could be part of an evolutionary strategy to increase viral fitness (76). For example, the species D Ad9 with a very short fiber was found to allow fiber-independent binding of the penton base directly to integrins, if integrins were present in sufficient amounts (51). In integrin-low cells, the virus instead used CAR for productive infection. Our findings that species B1 adenoviruses use avidity to bind to the CD46 receptor has important consequences for tropism and possibly evolution of the species B1 viruses, where viral receptor-binding proteins are under selective pressure and undergo constant variation to evade neutralization by antibodies (23, 47). High affinity binding could, for example, represent a dead-end in evolutionary terms, as such viruses would be constrained to a single receptor. Weak affinity to a receptor could be essential for gaining access to new attachment receptors.

Avidity captures low affinity interactions

Viruses use multiple binding strategies, characterized by a broad range of affinity interactions when analyzed for single binding interaction sites (22, 73). Viruses with low affinities include, e.g., influenza virus with millimolar affinity for sialic acid, and micromolar affinities for rhinovirus attachment to intercellular adhesion molecule-1, echovirus to decay-accelerating factor, or reovirus to junction adhesion molecule (2, 6, 28, 62). Biologically important binding of viruses to low affinity receptors occurs, when virus particles expose multiple binding sites. This allows for avidity effects and increases overall affinity.

Avidity is characterized by a synergistic (and not additive) combination of individual bond affinities, which largely depends on the structure and geometry of the involved molecules (36). For example, in the case of an IgG with a valency of two, avidity can lead to a strong increase of overall affinity, when compared to corresponding

monovalent Fab fragments (see e.g., an early study from 16). Particularly strong avidity effects were also reported for low affinity ErbB2-specific single chain variable fragment antibodies, where the antibody fragment with the lowest affinity showed highest avidity increase upon dimerization (44). Viruses containing trimeric attachment receptors, such as the reovirus sigma 1 protein or the long and short fibers of bacteriophage T4, have been suggested to employ avidity mechanisms for infection (as discussed in 33). Interestingly, binding of Ad3 to DSG-2 may engage avidity mechanism, since multimerization of the trimeric Ad3 FK was required for efficient binding to DSG-2 (69).

Avidity binding of adenoviruses to CD46 and CAR

Some studies considered Ad3/7 and also Ad14 to be CD46 non-binders due to low affinity interactions with CD46 (15, 19, 37, 56, 57, 67). Several lines of evidence, however, support an avidity-based mechanism for Ad3/7 infection of CD46 positive cells. First, Ad3/7 infection correlated with the levels of ectopically expressed CD46, while Ad11/35 infection was saturated at low CD46 expression levels. Second, the binding of species B Ad3/7-FK to immobilized CD46 on a biosensor chip was more dependent on the receptor density than binding of Ad11/35-FK, and the Ad3/7-FK binding had only 10-15 fold lower apparent affinity than Ad11/35-FK. Third, cross-linking of soluble CD46 increased its blocking effect on Ad3/7 infection in human A549 cells and CHO-CD46 cells. Fourth, soluble Ad3/7-FKs inefficiently blocked Ad3/7 infection of CHO-CD46 cells, unlike Ad11/35-FKs, which efficiently blocked all four tested B serotypes, confirming that Ad3/7 FKs bind with lower affinity to CD46 than Ad11/35 FKs. These data support and extend earlier binding site mapping studies, which showed that Ad3/7 engage CD46 through similar surfaces as species B2 Ad11/35 (13). In support of this, the recent SPR studies by Persson *et al.* revealed a broad variation of CD46 binding affinities, and the authors concluded that Ad7/11/14/35 are capable to bind to the same epitopes on CD46 (48). All these data are in accordance with the observations that both the low affinity CD46 binder Ad3 and the high affinity binder Ad35 use virtually identical pathways to infect human cells that are CD46-positive (1, 24). Notable, avidity mechanisms may also allow the

609 species B Ad16 to use CD46 for productive infection by increasing the affinity to
610 CD46 by 70-fold compared to Ad11 (47).

611 Similar to the species B serotypes, also the CAR-tropic species C Ad serotypes have
612 a broad spectrum of affinities to CAR over nearly 3 orders of magnitude, ranging from
613 the low affinity binder Ad9 to the high affinity binder Ad5 (25). In addition, avidity
614 effects could be measured by an increase of FK affinity from about 25 nM for
615 monomeric immobilized Ad2 FK to 1 nM for multivalent immobilized CAR in SPR
616 assays employing minimal-sized proteins produced in *E.coli* (33). The avidity-driven
617 multivalent binding reaction to immobilized high density CAR (200 RU equivalent to
618 our CD46 high density chips) could be fitted to a trivalent binding model. We thus
619 consider it likely that many different Ads use avidity binding for attachment and
620 possibly entry into cells.

621 Avidity effects for Ad–receptor interactions can occur at two levels. The trivalent FK
622 protein can increase the overall affinity compared to a monovalent protein. In
623 addition, the 12 fiber trimmers on the virus may simultaneously form multiple contact
624 points with the cell surface. Both of these mechanisms can contribute to increase the
625 overall affinities of the virus particle to its receptor. Importantly, in the case of the
626 CAR binders Ad2/5, CAR clustering leads to viral surfing motions on the cell surface
627 and triggers viral uncoating assisted by confined motions of the viral coreceptor alpha
628 v integrin (5).

629

630 **Apparent K_D values of species B FKs to divalent CD46 differ from K_D values**
631 **with monovalent soluble CD46**

632 Avidity effects are strongly dependent on the valency of the ligand, as observed for
633 example with binding of dimeric ephrin-A5 ligand to dimerized EphA3 receptor (45).
634 Accordingly, the measured K_D values for FKs to our CD46ex-Fc were about 5 logs
635 lower for the Ad3/7-FKs, and 3 logs lower for Ad11/35 compared to the K_D values for
636 the monovalent CD46-SCR I-II interactions published by others (10, 47, 48, 71, 72).
637 Further to the valency difference, the CD46-SCR I-II protein used in other studies
638 was produced in mutant CHO cells and contained homogenous, high mannose N-

linked carbohydrates (48). Our CD46 protein consisted of the entire extracellular domain plus a dimerizing Fc portion, and was produced in normal BHK cells allowing for complex O- and N-linked glycosylations (60). Interestingly, the extended CD46 SCR I-IV domain has a somewhat different binding mode to Ad11-FK, as the contact site did not include the IJ loop described for CD46 SCR I-II interaction (50). We suggest that the dimeric nature of our CD46ex-huFc explains why the binding of the Ad3/7/11/35 FKs fit better to a two-stage reaction model than to trivalent binding models, described earlier for Ad2-FK interaction with CAR (33). This is based on comparison of the different affinities under our standard conditions. We conclude that the observed K_D differences between the monovalent and trivalent affinities of the Ad3/7/11/35-FKs are based on avidity binding.

Virus–receptor affinity *versus* receptor density

A recent systematic study with retargeted MV vectors has shown that viruses displaying HER2/neu-specific single-chain variable fragment antibodies had high avidity and cell killing ability due to dozens of single chain molecules in the viral envelope, even if their single affinities were in the low micro-molar range (21). This study noticed a receptor threshold level for productive infection, together with an inverse correlation of attachment receptor affinity and receptor density requirements for infection. In particular, supra-threshold affinities did not further enhance the efficiency of MV infection, which corresponds well with our results for high affinity CD46 binders Ad11/35. It also fits well with another observation showing that Ad35-FK mutants with either 4-fold or 60-fold higher affinity at the monovalent interaction level did not yield higher transduction levels, regardless of the cellular CD46 receptor density (72).

With the FK neutralization experiments in CHO-CD46#2 expressing cells, we noticed that Ad3/7-FKs did not efficiently compete against the binding of corresponding virus particles, in contrast to Ad11/35-FKs, which efficiently blocked Ad3/7/11/35. This is due to low affinity of Ad3/7-FK for CD46, since binding of the different species B Ads is restricted to CD46 in these cells (13, 60). This conclusion was corroborated by the

findings that soluble CD46ex-huFc inefficiently inhibited binding of Ad3/7 to the cells, in agreement with weak blocking efficiency of Ad3/7 by soluble CD46 (13, 67), and also by soluble monovalent CD46 for MV infection (58). Ad3/7 inhibition was, however, strongly enhanced by cross-linking the CD46ex-huFc protein (Fig. 3), suggesting that cross-linked CD46ex-huFc mimics the multiple interaction situation when the virus contacts the cell surface. Similarly, CD46 cross-linking by genetically fusing the CD46 ectodomain to the octamer oligomerization domain of C4b binding protein resulted in a 2 log enhanced MV neutralizing activity *in vitro* and *in vivo* due to enhanced virus binding (8).

These data suggest that the receptor density is of key importance not only for interaction of CD46 with trimeric FK, but also the multivalent virus particle. Together or alone, this gives rise to avidity effects, which allow Ad3/7 to infect cells expressing sufficient levels of CD46 (13, 20, 60). The lack of Ad3/7 infection in CHO-CD46 cells reported by other groups is most likely due to low CD46 expression levels, and assay systems of low sensitivity or limited dynamic range (15, 18, 37, 57, 67).

Mechanistic implications of desmoglein-2 and CD46 as receptors for Ad3/7

Our DSG-2/CD46 combinatorial loss-of-function experiments in A549 and 16HBE14o cells significantly enhanced the reduction of cell surface binding and infection of Ad3 by ~ 10% compared to DSG-2 interference alone, showing that CD46 has a significant role for infectious Ad3 entry in these cells. We suggest that in non-polarized A549, 16HBE14o or HeLa cells (70) expressing both receptors, DSG-2 functions as a major attachment receptor for Ad3. This could be due to a lower affinity/avidity of Ad3 to CD46 compared to DSG-2, or to higher levels of DSG-2 compared to CD46. In other human cells the CD46 contribution may be more pronounced depending on the expression levels of the receptors. This is supported by our data from rodent CHO-CD46 and human M010119 melanoma cells lacking DSG-2, where Ad3/7 uses CD46 as functional receptor.

For oncolytic therapies with HAdVs, it will be important to determine the DSG-2 expression levels among human cells and tissues in health and disease and put

these data in relation to CD46 expression. In particular, it is conceivable that DSG-2 and CD46 act independently as Ad3/7 receptors. For example in polarized cells, DSG-2 is a component of the cell-cell adhesion structure of intercellular junctions (26). CD46 is present on apical and basolateral surfaces (3, 59, 64). Apical CD46 may be an initial docking site for species B HAdVs, and lead to the activation of DSG-2 from the lateral cell-cell contact sites. Interestingly, a library screening experiment of fiber-pseudotyped Ads revealed relatively high levels of apical transduction of Caco-2 cells by Ad7 and Ad35, despite low levels of virus attachment to the apical membrane (29). Speculatively, apical infections may be exacerbated by cytokine-mediated relocalization of CD46 and DSG-2 to the apical surface upon cytokine signaling from immune cells, as demonstrated for species C receptors CAR and alpha v beta 3 integrins (35). This may lead to a situation where DSG-2 and CD46 complement each other, for example by physical interactions. Possibly, DSG-2 or another molecule function as a tethering factor for CD46, and prolong the half-life of CD46 on the plasma membrane thereby increasing the CD46 avidity effects. Clustering of CD46 may occur in particular lipid domains (66) or in the vicinity of integrins or tetraspanins (34). In this scenario, lipids, integrins or tetraspannins could be modulators for CD46 function, and may not be required for Ad3 infection, if the CD46 levels were sufficiently high. Clustering of CD46 by antibodies or Ad3/35 facilitates CD46 internalization by clathrin-mediated endocytosis or macropinocytosis, followed by endosome lysis in the case of Ad3/35 and virus particle penetration from endosomes to the cytosol (1, 9, 24).

Acknowledgements

We thank Leta Fuchs for technical assistance, Richard Sutton (Baylor College of Medicine, Houston Texas) for providing the pBlasti lentiviral vector system, Denis Gerlier (Université Lyon, Lyon, France, for providing the MCI20.6 anti-CD46 hybridoma), Dr. Dieter Gruenert (California Pacific Medical Center Research Institute, University of California, San Francisco) for providing 16HBE14o cells, and the FACS Core Facility Irchel from the University of Zurich for cell sorting service. We also thank for Dr. Johan Hoebeke, Kessel-Lo, Belgium for providing the equations and algorithms to evaluate the SPR data with trivalent binding model. This work was supported by the Kanton Zürich (SH, UFG) and by the grant 31003A-116856 of the Swiss National Science Foundation (SH).

References

1. **Amstutz, B., M. Gastaldelli, S. Kalin, N. Imelli, K. Boucke, E. Wandeler, J. Mercer, S. Hemmi, and U. F. Greber.** 2008. Subversion of CtBP1-controlled macropinocytosis by human adenovirus serotype 3. EMBO J **27:**956-69.

2. **Barton, E. S., J. C. Forrest, J. L. Connolly, J. D. Chappell, Y. Liu, F. J. Schnell, A. Nusrat, C. A. Parkos, and T. S. Dermody.** 2001. Junction adhesion molecule is a receptor for reovirus. Cell **104:**441-51.

3. **Blau, D. M., and R. W. Compans.** 1995. Entry and release of measles virus are polarized in epithelial cells. Virology **210:**91-9.

4. **Buchholz, C. J., U. Schneider, P. Devaux, D. Gerlier, and R. Cattaneo.** 1996. Cell entry by measles virus: long hybrid receptors uncouple binding from membrane fusion. J Virol **70:**3716-23.

5. **Burckhardt, C. J., M. Suomalainen, P. Schoenenberger, K. Boucke, S. Hemmi, and U. F. Greber.** 2011. Drifting Motions of the Adenovirus Receptor CAR and Immobile Integrins Initiate Virus Uncoating and Membrane Lytic Protein Exposure. Cell Host Microbe **10:**105-17.

6. **Casasnovas, J. M., and T. A. Springer.** 1995. Kinetics and thermodynamics of virus binding to receptor. Studies with rhinovirus, intercellular adhesion molecule-1 (ICAM-1), and surface plasmon resonance. J Biol Chem **270:**13216-24.

7. **Chmielewicz, B., J. Benzler, G. Pauli, G. Krause, F. Bergmann, and B. Schweiger.** 2005. Respiratory disease caused by a species B2 adenovirus in a military camp in Turkey. J Med Virol **77:**232-7.

8. **Christiansen, D., P. Devaux, B. Reveil, A. Evlashev, B. Horvat, J. Lamy, C. Rabourdin-Combe, J. H. Cohen, and D. Gerlier.** 2000. Octamerization enables soluble CD46 receptor to neutralize measles virus in vitro and in vivo. J Virol **74:**4672-8.

9. **Crimeen-Irwin, B., S. Ellis, D. Christiansen, M. J. Ludford-Menting, J. Milland, M. Lanteri, B. E. Loveland, D. Gerlier, and S. M. Russell.** 2003. Ligand binding determines whether CD46 is internalized by clathrin-coated pits or macropinocytosis. J. Biol. Chem. **278:**46927-46937.

10. **Cupelli, K., S. Muller, B. D. Persson, M. Jost, N. Arnberg, and T. Stehle.** 2010. Structure of adenovirus type 21 knob in complex with CD46 reveals key differences in receptor contacts among species B adenoviruses. J Virol **84:**3189-200.

11. **Durmort, C., C. Stehlin, G. Schoehn, A. Mitraki, E. Drouet, S. Cusack, and W. P. Burmeister.** 2001. Structure of the fiber head of Ad3, a non-CAR-binding serotype of adenovirus. Virology **285:**302-12.

12. **Ebbinghaus, C., A. Al-Jaibaji, E. Operschall, A. Schoffel, I. Peter, U. F. Greber, and S. Hemmi.** 2001. Functional and selective targeting of adenovirus to high-affinity Fcgamma receptor I-positive cells by using a bispecific hybrid adapter. J Virol **75:**480-9.

13. **Fleischli, C., D. Sirena, G. Lesage, M. J. Havenga, R. Cattaneo, U. F. Greber, and S. Hemmi.** 2007. Species B adenovirus serotypes 3, 7, 11 and

35 share similar binding sites on the membrane cofactor protein CD46 receptor. J Gen Virol **88:**2925-34.

14. **Fleischli, C., S. Verhaagh, M. Havenga, D. Sirena, W. Schaffner, R. Cattaneo, U. F. Greber, and S. Hemmi.** 2005. The distal short consensus repeats 1 and 2 of the membrane cofactor protein CD46 and their distance from the cell membrane determine productive entry of species B adenovirus serotype 35. J Virol **79:**10013-10022.

15. **Gaggar, A., D. M. Shayakhmetov, and A. Lieber.** 2003. CD46 is a cellular receptor for group B adenoviruses. Nat Med **9:**1408-12.

16. **Greenbury, C. L., D. H. Moore, and L. A. Nunn.** 1965. The Reaction with Red Cells of 7s Rabbit Antibody, Its Sub-Units and Their Recombinants. Immunology **8:**420-31.

17. **Gruenert, D. C., C. B. Basbaum, and J. H. Widdicombe.** 1990. Long-term culture of normal and cystic fibrosis epithelial cells grown under serum-free conditions. In Vitro Cell Dev Biol **26:**411-8.

18. **Gustafsson, B., W. Huang, G. Bogdanovic, F. Gauffin, A. Nordgren, G. Talekar, D. A. Ornelles, and L. R. Gooding.** 2007. Adenovirus DNA is detected at increased frequency in Guthrie cards from children who develop acute lymphoblastic leukaemia. Br J Cancer **97:**992-4.

19. **Gustafsson, D. J., A. Segerman, K. Lindman, Y. F. Mei, and G. Wadell.** 2006. The Arg279Gln [corrected] substitution in the adenovirus type 11p (Ad11p) fiber knob abolishes EDTA-resistant binding to A549 and CHO-CD46 cells, converting the phenotype to that of Ad7p. J Virol **80:**1897-905.

20. **Hall, K., M. E. Blair Zajdel, and G. E. Blair.** 2009. Defining the role of CD46, CD80 and CD86 in mediating adenovirus type 3 fiber interactions with host cells. Virology **392:**222-9.

21. **Hasegawa, K., C. Hu, T. Nakamura, J. D. Marks, S. J. Russell, and K. W. Peng.** 2007. Affinity thresholds for membrane fusion triggering by viral glycoproteins. J Virol **81:**13149-57.

22. **Helenius, A.** 2007. Virus entry and uncoating, p. 99-118. *In* D. M. Knipe and P. M. Howley (ed.), Fields Virology, vol. 1. Walters Kluwer, Lippincott Williams & Wilkins, Philadelphia, Baltimore, New York, London, Buenos Aires, Hong Kong, Sydney, Tokyo.

23. **Howitt, J., C. W. Anderson, and P. Freimuth.** 2003. Adenovirus interaction with its cellular receptor CAR. Curr Top Microbiol Immunol **272:**331-64.

24. **Kalin, S., B. Amstutz, M. Gastaldelli, N. Wolfrum, K. Boucke, M. Havenga, F. DiGennaro, N. Liska, S. Hemmi, and U. F. Greber.** 2010. Macropinocytotic uptake and infection of human epithelial cells with species B2 adenovirus type 35. J Virol **84:**5336-50.

25. **Kirby, I., R. Lord, E. Davison, T. J. Wickham, P. W. Roelvink, I. Kovesdi, B. J. Sutton, and G. Santis.** 2001. Adenovirus type 9 fiber knob binds to the coxsackie B virus-adenovirus receptor (CAR) with lower affinity than fiber knobs of other CAR-binding adenovirus serotypes. J Virol **75:**7210-4.

26. **Kowalczyk, A. P., T. S. Stappenbeck, D. A. Parry, H. L. Palka, M. L. Virata, E. A. Bornslaeger, L. A. Nilles, and K. J. Green.** 1994. Structure and

function of desmosomal transmembrane core and plaque molecules. Biophys Chem **50:**97-112.

27. **Kumar, M., B. Keller, N. Makalou, and R. E. Sutton.** 2001. Systematic determination of the packaging limit of lentiviral vectors. Hum Gene Ther **12:**1893-905.

28. **Lea, S. M., R. M. Powell, T. McKee, D. J. Evans, D. Brown, D. I. Stuart, and P. A. van der Merwe.** 1998. Determination of the affinity and kinetic constants for the interaction between the human virus echovirus 11 and its cellular receptor, CD55. J Biol Chem **273:**30443-7.

29. **Lecollinet, S., F. Gavard, M. J. Havenga, O. B. Spiller, A. Lemckert, J. Goudsmit, M. Eloit, and J. Richardson.** 2006. Improved gene delivery to intestinal mucosa by adenoviral vectors bearing subgroup B and d fibers. J Virol **80:**2747-59.

30. **Leen, A. M., and C. M. Rooney.** 2005. Adenovirus as an emerging pathogen in immunocompromised patients. Br J Haematol **128:**135-44.

31. **Lemckert, A. A., J. Grimbergen, S. Smits, E. Hartkoorn, L. Holterman, B. Berkhout, D. H. Barouch, R. Vogels, P. Quax, J. Goudsmit, and M. J. Havenga.** 2006. Generation of a novel replication-incompetent adenoviral vector derived from human adenovirus type 49: manufacture on PER.C6 cells, tropism and immunogenicity. J Gen Virol **87:**2891-9.

32. **Lewis, P. F., M. A. Schmidt, X. Lu, D. D. Erdman, M. Campbell, A. Thomas, P. R. Cieslak, L. D. Grenz, L. Tsaknardis, C. Gleaves, B. Kendall, and D. Gilbert.** 2009. A community-based outbreak of severe respiratory illness caused by human adenovirus serotype 14. J Infect Dis **199:**1427-34.

33. **Lortat-Jacob, H., E. Chouin, S. Cusack, and M. J. van Raaij.** 2001. Kinetic analysis of adenovirus fiber binding to its receptor reveals an avidity mechanism for trimeric receptor-ligand interactions. J Biol Chem **276:**9009-15.

34. **Lozahic, S., D. Christiansen, S. Manie, D. Gerlier, M. Billard, C. Boucheix, and E. Rubinstein.** 2000. CD46 (membrane cofactor protein) associates with multiple beta1 integrins and tetraspans. Eur. J. Immunol. **30:**900-907.

35. **Lutschg, V., K. Boucke, S. Hemmi, and U. F. Greber.** 2011. Chemotactic antiviral cytokines promote infectious apical entry of human adenovirus into polarized epithelial cells. Nat Commun **2:**391.

36. **Mammen, M., S. Choi, and G. M. Whitesides.** 1998. Polyvalent Interactions in Biological Systems: Implications for Design and Use of Multivalent Ligands and Inhibitiors. Angewandte Chemie International Edition **37:**2754-94.

37. **Marttila, M., D. Persson, D. Gustafsson, M. K. Liszewski, J. P. Atkinson, G. Wadell, and N. Arnberg.** 2005. CD46 is a cellular receptor for all species B adenoviruses except types 3 and 7. J Virol **79:**14429-36.

38. **Meier, O., M. Gastaldelli, K. Boucke, S. Hemmi, and U. F. Greber.** 2005. Early steps of clathrin-mediated endocytosis involved in phagosomal escape of Fcgamma receptor-targeted adenovirus. J. Virol. **79:**2604-2613.

39. **Metzgar, D., M. Osuna, A. E. Kajon, A. W. Hawksworth, M. Irvine, and K. L. Russell.** 2007. Abrupt emergence of diverse species B adenoviruses at US military recruit training centers. J Infect Dis **196:**1465-73.

40. **Murakami, M., H. Ugai, M. Wang, N. Belousova, P. Dent, P. B. Fisher, J. N. Glasgow, M. Everts, and D. T. Curiel.** 2010. An adenoviral vector expressing human adenovirus 5 and 3 fiber proteins for targeting heterogeneous cell populations. Virology **407:**196-205.

41. **Myszka, D. G.** 1999. Improving biosensor analysis. J Mol Recognit **12:**279-84.

42. **Naniche, D., G. Varior-Krishnan, F. Cervoni, T. F. Wild, B. Rossi, C. Rabourdin-Combe, and D. Gerlier.** 1993. Human membrane cofactor protein (CD46) acts as a cellular receptor for measles virus. J Virol **67:**6025-32.

43. **Nemerow, G. R., L. Pache, V. Reddy, and P. L. Stewart.** 2009. Insights into adenovirus host cell interactions from structural studies. Virology **384:**380-8.

44. **Nielsen, U. B., G. P. Adams, L. M. Weiner, and J. D. Marks.** 2000. Targeting of bivalent anti-ErbB2 diabody antibody fragments to tumor cells is independent of the intrinsic antibody affinity. Cancer Res **60:**6434-40.

45. **Pabbisetty, K. B., X. Yue, C. Li, J. P. Himanen, R. Zhou, D. B. Nikolov, and L. Hu.** 2007. Kinetic analysis of the binding of monomeric and dimeric ephrins to Eph receptors: correlation to function in a growth cone collapse assay. Protein Sci **16:**355-61.

46. **Pache, L., S. Venkataraman, G. R. Nemerow, and V. S. Reddy.** 2008. Conservation of fiber structure and CD46 usage by subgroup B2 adenoviruses. Virology **375:**573-9.

47. **Pache, L., S. Venkataraman, V. S. Reddy, and G. R. Nemerow.** 2008. Structural variations in species B adenovirus fibers impact CD46 association. J Virol **82:**7923-31.

48. **Persson, B. D., S. Muller, D. M. Reiter, B. B. Schmitt, M. Marttila, C. V. Sumowski, S. Schweizer, U. Scheu, C. Ochsenfeld, N. Arnberg, and T. Stehle.** 2009. An arginine switch in the species B adenovirus knob determines high-affinity engagement of cellular receptor CD46. J Virol **83:**673-86.

49. **Persson, B. D., D. M. Reiter, M. Marttila, Y. F. Mei, J. M. Casasnovas, N. Arnberg, and T. Stehle.** 2007. Adenovirus type 11 binding alters the conformation of its receptor CD46. Nat Struct Mol Biol **14:**164-6.

50. **Persson, B. D., N. B. Schmitz, C. Santiago, G. Zocher, M. Larvie, U. Scheu, J. M. Casasnovas, and T. Stehle.** 2010. Structure of the extracellular portion of CD46 provides insights into its interactions with complement proteins and pathogens. PLoS Pathog **6**.

51. **Roelvink, P. W., I. Kovesdi, and T. J. Wickham.** 1996. Comparative analysis of adenovirus fiber-cell interaction: adenovirus type 2 (Ad2) and Ad9 utilize the same cellular fiber receptor but use different binding strategies for attachment. J Virol **70:**7614-21.

52. **Sakurai, F., K. Kawabata, and H. Mizuguchi.** 2007. Adenovirus vectors composed of subgroup B adenoviruses. Curr Gene Ther **7:**229-38.

53. **Sakurai, F., S. Murakami, K. Kawabata, N. Okada, A. Yamamoto, T. Seya, T. Hayakawa, and H. Mizuguchi.** 2006. The short consensus repeats 1 and 2, not the cytoplasmic domain, of human CD46 are crucial for infection of subgroup B adenovirus serotype 35. J Control Release **113:**271-8.

54. **Schmitz, H., R. Wigand, and W. Heinrich.** 1983. Worldwide epidemiology of human adenovirus infections. Am J Epidemiol **117:**455-66.

55. **Schmitz, M., C. Graf, T. Gut, D. Sirena, I. Peter, R. Dummer, U. F. Greber, and S. Hemmi.** 2006. Melanoma cultures show different susceptibility towards E1A-, E1B-19 kDa- and fiber-modified replication-competent adenoviruses. Gene Ther **13:**893-905.

56. **Segerman, A., N. Arnberg, A. Erikson, K. Lindman, and G. Wadell.** 2003. There are two different species B adenovirus receptors: sBAR, common to species B1 and B2 adenoviruses, and sB2AR, exclusively used by species B2 adenoviruses. J. Virol. **77:**1157-1162.

57. **Segerman, A., J. P. Atkinson, M. Marttila, V. Dennerquist, G. Wadell, and N. Arnberg.** 2003. Adenovirus type 11 uses CD46 as a cellular receptor. J Virol **77:**9183-91.

58. **Seya, T., M. Kurita, T. Hara, K. Iwata, T. Semba, M. Hatanaka, M. Matsumoto, Y. Yanagi, S. Ueda, and S. Nagasawa.** 1995. Blocking measles virus infection with a recombinant soluble form of, or monoclonal antibodies against, membrane cofactor protein of complement (CD46). Immunology **84:**619-25.

59. **Sinn, P. L., G. Williams, S. Vongpunsawad, R. Cattaneo, and P. B. McCray, Jr.** 2002. Measles virus preferentially transduces the basolateral surface of well-differentiated human airway epithelia. J. Virol. **76:**2403-2409.

60. **Sirena, D., B. Lilienfeld, M. Eisenhut, S. Kalin, K. Boucke, R. R. Beerli, L. Vogt, C. Ruedl, M. F. Bachmann, U. F. Greber, and S. Hemmi.** 2004. The Human Membrane Cofactor CD46 Is a Receptor for Species B Adenovirus Serotype 3. J Virol **78:**4454-4462.

61. **Sirena, D., Z. Ruzsics, W. Schaffner, U. F. Greber, and S. Hemmi.** 2005. The nucleotide sequence and a first generation gene transfer vector of species B human adenovirus serotype 3. Virology **343:**283-98.

62. **Skehel, J. J., and D. C. Wiley.** 2000. Receptor binding and membrane fusion in virus entry: the influenza hemagglutinin. Annu Rev Biochem **69:**531-69.

63. **Stecher, H., D. M. Shayakhmetov, G. Stamatoyannopoulos, and A. Lieber.** 2001. A capsid-modified adenovirus vector devoid of all viral genes: assessment of transduction and toxicity in human hematopoietic cells. Mol. Ther. **4:**36-44.

64. **Strauss, R., P. Sova, Y. Liu, Z. Y. Li, S. Tuve, D. Pritchard, P. Brinkkoetter, T. Moller, O. Wildner, S. Pesonen, A. Hemminki, N. Urban, C. Drescher, and A. Lieber.** 2009. Epithelial phenotype confers resistance of ovarian cancer cells to oncolytic adenoviruses. Cancer Res **69:**5115-25.

65. **Suomalainen, M., M. Y. Nakano, S. Keller, K. Boucke, R. P. Stidwill, and U. F. Greber.** 1999. Microtubule-dependent plus- and minus end-directed motilities are competing processes for nuclear targeting of adenovirus. J. Cell. Biol. **144:**657-672.

66. **Tang, H., A. Kawabata, M. Takemoto, K. Yamanishi, and Y. Mori.** 2008. Human herpesvirus-6 infection induces the reorganization of membrane

microdomains in target cells, which are required for virus entry. Virology **378:**265-71.

67. **Tuve, S., H. Wang, C. Ware, Y. Liu, A. Gaggar, K. Bernt, D. Shayakhmetov, Z. Li, R. Strauss, D. Stone, and A. Lieber.** 2006. A new group B adenovirus receptor is expressed at high levels on human stem and tumor cells. J Virol **80:**12109-20.

68. **Wadell, G.** 2000. Adenoviruses, p. 307-327. *In* A. J. Zuckerman, J. E. Banatvala, and J. R. Pattison (ed.), Principles and Practice of Clinical Virology, Fourth Edition ed. John Wiley & Sons, Ltd.

69. **Wang, H., Z. Li, R. Yumul, S. Lara, A. Hemminki, P. Fender, and A. Lieber.** 2011. Multimerization of adenovirus serotype 3 fiber knob domains is required for efficient binding of virus to desmoglein 2 and subsequent opening of epithelial junctions. J Virol **85:**6390-402.

70. **Wang, H., Z. Y. Li, Y. Liu, J. Persson, I. Beyer, T. Moller, D. Koyuncu, M. R. Drescher, R. Strauss, X. B. Zhang, J. K. Wahl, 3rd, N. Urban, C. Drescher, A. Hemminki, P. Fender, and A. Lieber.** 2011. Desmoglein 2 is a receptor for adenovirus serotypes 3, 7, 11 and 14. Nat Med **17:**96-104.

71. **Wang, H., Y. C. Liaw, D. Stone, O. Kalyuzhniy, I. Amiraslanov, S. Tuve, C. L. Verlinde, D. Shayakhmetov, T. Stehle, S. Roffler, and A. Lieber.** 2007. Identification of CD46 binding sites within the adenovirus serotype 35 fiber knob. J Virol **81:**12785-92.

72. **Wang, H., Y. Liu, Z. Li, S. Tuve, D. Stone, O. Kalyushniy, D. Shayakhmetov, C. L. Verlinde, T. Stehle, J. McVey, A. Baker, K. W. Peng, S. Roffler, and A. Lieber.** 2008. In vitro and in vivo properties of adenovirus vectors with increased affinity to CD46. J Virol **82:**10567-79.

73. **Wang, J.** 2002. Protein recognition by cell surface receptors: physiological receptors versus virus interactions. Trends Biochem Sci **27:**122-6.

74. **Wu, E., S. A. Trauger, L. Pache, T. M. Mullen, D. J. von Seggern, G. Siuzdak, and G. R. Nemerow.** 2004. Membrane cofactor protein is a receptor for adenoviruses associated with epidemic keratoconjunctivitis. J Virol **78:**3897-905.

75. **Zacharias, D. A., J. D. Violin, A. C. Newton, and R. Y. Tsien.** 2002. Partitioning of lipid-modified monomeric GFPs into membrane microdomains of live cells. Science **296:**913-6.

76. **Zhang, Y., and J. M. Bergelson.** 2005. Adenovirus receptors. J Virol **79:**12125-31.

77. **Zhu, Z., Y. Zhang, S. Xu, P. Yu, X. Tian, L. Wang, Z. Liu, L. Tang, N. Mao, Y. Ji, C. Li, Z. Yang, S. Wang, J. Wang, D. Li, and W. Xu.** 2009. Outbreak of acute respiratory disease in China caused by B2 species of adenovirus type 11. J Clin Microbiol **47:**697-703.

998 **Legends to figures**

999 **Fig. 1.** Loss-of-function studies for individual contribution of CD46 and DSG-2 to Ad3
1000 infection. (A, B) Inhibition of Ad3 (A) and Ad35 (B) binding to A549 cells by anti-
1001 CD46 and DSG-2 antibodies. A549 cells were incubated with the indicated
1002 concentrations of CD46 (MEM258), DSG-2 (6D8 and 8E5), a mix of both types of
1003 antibodies, control CAR antibodies or PBS, followed by the addition of atto-488-
1004 labeled Ad3 or Ad35 at 4°C. Virus binding was assesed by cytofluorometric analysis.
1005 The data were normalized to the amounts of virus bound when using PBS. Mean
1006 values and standard deviations of triplicates from one representative experiment are
1007 shown. (C-H) Effect of siRNA-mediated down-regulation on virus infection in A549
1008 (C-E) and 16HBE14o cells (F-H). (C, F) Cells were transfected with the indicated
1009 siRNAs resulting in specific down-regulation of CD46 and DSG-2, but not of
1010 unrelated CAR. Shown is one representative analysis. (D, G) Binding of atto488-
1011 labeled Ad2 (control), Ad3 and Ad35 to siRNA-transfected cells was assessed as
1012 described above. (E, H) Transduction of siRNA-transfected cells with eGFP
1013 expressing control Ad5, Ad3 and Ad35 vectors at 500 vp/cell. eGFP expression
1014 values were analyzed two days p.i. by flow cytometry and are expressed as mean
1015 fluorescence intensity values (MFI).

1016

1017 **Fig. 2.** Binding and transduction of adenovirus species B viruses in CD46 gain-of-
1018 function cells negative for DSG-2. (A) For Ad binding assays, 5 x 10^5 of human A549
1019 cells, and the different rodent CHO-CD46 cells were incubated on ice with 1,000 vp
1020 of the indicated [^{3}H]-labeled species B serotypes. After incubation for 2 h, the cells
1021 were washed and cell-associated radioactivity was determined. Mean values and
1022 standard deviations of triplicates from one representative experiment are shown.
1023 Asterisks indicate here and in the experiments below the level of significance
1024 (*P<0.05; **P<0.005; ***P<0.0005 for comparisons of corresponding Ad binding
1025 (infection) in parental CHO versus CD46-transfected cells). (B) Transduction assays
1026 of human A549, parental CHO and CHO-CD46 expressing cells. 10^5 cells were
1027 incubated with eGFP expressing Ad3, Ad7, Ad11, and Ad35 vectors at increasing
1028 virus concentrations of 10, 100, and 1,000 vp/cell. eGFP expression was analyzed

two days p.i. by flow cytometry and are expressed as MFI. (C) Transduction assays of human parental and stable CD46-transfected M010119 melanoma cells. Cells were transduced and tested as described above. Background fluorescence intensity for uninfected M010191-eGFP-CD46 cells was higher due to the eGFP-tagged CD46 in these cells.

Fig. 3. Cross-linking of CD46ex-huFc strongly increases blocking of Ad3/7 infection in CHO-CD46#2 and A549 cells. (A) CHO-CD46#2 cells or (B) A549 cells were pre-incubated for 1 h in the cold using the indicated concentrations of adapter CD46ex-huFc alone or in combination with a 2-fold increase series of goat-anti human Fc antibody. Following addition of the different eGFP-expressing vectors for another 1 h, cells were washed and analyzed 48 h p.i. Asterisks indicate the level of significance (*P<0.05; **P<0.005; ***P<0.0005 for comparisons of corresponding Ad infection using CD46ex-huFc versus control CARex-huFc of sFig. 2).

Fig. 4. Inhibition of Ad3-, Ad7-, Ad11-, and Ad35-eGFP transduction in CHO-CD46#2 and A549 cells by recombinant Ad fiber knobs. Cells were pre-incubated for 1 h in the cold using a 5-fold dilution series of the individual FK proteins, followed by addition of the different eGFP-expressing vectors for another 1 h. (A) For CHO-CD46#2 cells, the viral inputs amounted to 29,600, 8,200, 657, and 1,088 vp / cell for Ad3-, Ad7-, Ad11-, and Ad35-eGFP, respectively. The virus input concentrations had been determined in preceding experiments and were chosen such that the unblocked transgene expression values amounted to fluorescence intensity values of about 200. eGFP analysis was performed 48 h p.i.. FKs are color-coded as follows: Ad5-FK in green, Ad3-FK in red, Ad7-FK in purple, Ad11-FK in cyan and Ad35-FK in dark blue. (B) For A549 cells virus inputs amounted to 14,800, 8,200, 1,314, 2,540 and 2,825 vp/cell for Ad3-, Ad7-, Ad11-, Ad35-, and Ad5-eGFP, respectively. Otherwise, the procedure was the same as above.

Fig. 5. Subtracted SPR sensograms for Ad3-, Ad7-, Ad11- and Ad35-FK interacting with CD46. Soluble receptor CD46ex-huFc was immobilized on a CM5 chip at high density in Fc2 (2,630 RU, 1, 3) and low density in Fc4 (345 RU, 2, 4). Control CARex-huFc was immobilized at high density in Fc1 (3,431 RU, 1, 3) and low density in Fc3 (278 RU, 2, 4). (A) to (D), FK analytes were injected over the sensor surface at 18.75 and 150 nM concentrations for Ad3-FK (A), Ad11-FK (C) and Ad35-FK (D), and at 11.07 and 88.59 nM for Ad7-FK (B), respectively. Association times were either 240 or 280 s. (E) to (H), overlay of analyte responses for Ad3-, Ad7-, Ad11- and Ad35-FK at different concentrations. Measurements were performed using the CD46 high-density 2,630 RU CM5 chip. Serial concentrations of 0.27, 0.82, 2.47, 7.41, 22.22 and 66.67 nM of Ad3-FK (E), Ad7-FK (F), Ad11-FK (G), and Ad35-FK (H) were injected in HBS-P+ buffer at 30 µl/min under contact time of 300 s and dissociation time of 3,600 s (for better visibility only four of the six binding curves are shown). Data evaluation was fitted globally by two-stage reaction model with Biacore T100 evaluation software, and resulting kinetics/affinity results are listed in sTable 1 and summarized in Table 4.

Table 1. Species B serotype-mediated eGFP transgene expression in different CHO-CD46-expressing cells compared to parental CHO and human A549 cells

	eGFP expression levels: Fold change compared to CHO[a]		
	CHO-CD46#6	CHO-CD46#1	CHO-CD46#2
Ad3-eGFP	18	55	192
Ad7-eGFP	37	85	354
Ad11-eGFP	40	88	79
Ad35-eGFP	60	106	96

	eGFP expression levels: % of A549 expression[b]			
	CHO	CHO-CD46#6	CHO-CD46#1	CHO-CD46#2
Ad3-eGFP	0.24	19	60	211
Ad7-eGFP	0.23	21	50	202
Ad11-eGFP	1.03	49	105	95
Ad35-eGFP	2.66	177	305	284

	eGFP expression levels: vp/cell needed to reach MFI 100[c]			
	CHO-CD46#6	CHO-CD46#1	CHO-CD46#2	A549
Ad3-eGFP	8,207 (27)	2,597 (16)	717 (4.2)	1,513 (2.7)
Ad7-eGFP	2,919 (9.5)	1,210 (7.3)	267 (1.57)	602 (1.1)
Ad11-eGFP	634 (2.1)	291 (1.8)	314 (1.8)	329 (0.6)
Ad35-eGFP	307	165	170	562

[a] Ratio of eGFP mean fluorescence intensity levels from CD46-expressing cell line to parental CHO were determined for 1,000 vp/cell input.

[b] Percentage of eGFP mean fluorescence intensity levels of CD46-expressing cells relative to A549 cells were determined for 1,000 vp/cell input.

[c] Regression lines were calculated for the eGFP expression levels; numbers in parentheses correspond to fold-higher virus concentration input compared to Ad35-eGFP.

Table 2. eGFP transgene expression analysis in M010119 and M010119-eGFP-CD46#8 cells

	eGFP expression levels: Fold change compared to M010119[a]	eGFP expression levels: vp/cell needed to reach MFI 100[b]	
		M010119	M010119-eGFP-CD46#8
Ad3-eGFP	86	34,513	271 (127)
Ad7-eGFP	26	4,695	91 (52)
Ad11-eGFP	2.1	344	110 (3.1)
Ad35-eGFP	2.3	258	130 (2.0)

[a] Ratio of eGFP mean fluorescence intensity levels from M010119-eGFP-CD46#8 cells to parental M010119 cells were determined for 1,000 vp/cell input.

[b] Regression lines were calculated for the eGFP expression levels. Numbers in parenthesis correspond to fold-enhancement of transduction efficiency in M010119-eGFP-CD46#8 cells compared to M010119 cells, based on MFI 100 values.

Table 3. Inhibition of Ad3/7/11/35-eGFP and Ad5-eGFP-mediated reporter expression by fiber knob cross-competition.

Competitor	Cells	% Inhibition of eGFP expression [a]				
		Ad3-eGFP	Ad7-eGFP	Ad11-eGFP	Ad35-eGFP	Ad5-eGFP
Ad3-FK	CHO-CD46	40	7	18	-3	nd
	A549	93	78	28	18	17/-9
Ad7-FK	CHO-CD46	86	81	21	-10	nd
	A549	95	87	4	-18	2/12
Ad11-FK	CHO-CD46	99	98	99	97	nd
	A549	93	95	99	100	-10/-6
Ad35-FK	CHO-CD46	98	85	97	96	nd
	A549	74	56	99	99	-1/-7
Ad5-FK	CHO-CD46	1	-35	16	0	nd
	A549	24	9	-21	29	26/97
		FK concentration for 50% inhibition (ng/ml) [b]				
		Ad3-eGFP	Ad7-eGFP	Ad11-eGFP	Ad35-eGFP	Ad5-eGFP
Ad3-FK	CHO-CD46	nd	nd	nd	nd	nd
	A549	25	23	nd	nd	nd
Ad7-FK	CHO-CD46	169	2'690	nd	nd	nd
	A549	17	31	nd	nd	nd
Ad11-FK	CHO-CD46	14	21	22	37	nd
	A549	31	87	13	14	nd
Ad35-FK	CHO-CD46	5	63	14	26	nd
	A549	470	4,459	33	5	105

[a]Data correspond to inhibitions obtained using 5,000 ng/ml FK concentration in Fig. 2C, D.

[b]Data were calculated by applying regression lines to values in Fig. 2C, D. nd: not determined.

Table 4. Summary kinetics/affinity analyses of Ad-FKs binding to immobilized CD46ex-huFc

	k_{a1} ($M^{-1}s^{-1}$)	k_{d1} (s^{-1})	k_{a2} (s^{-1})	k_{d2} (s^{-1})	$K_D \pm$ SEM (M)
Ad3-FK	2.30×10^{5}	6.88×10^{-4}	2.01×10^{-3}	1.76×10^{-4}	$2.48 \pm 0.27 \times 10^{-10}$
Ad7-FK	1.44×10^{5}	4.19×10^{-4}	1.94×10^{-3}	1.99×10^{-4}	$3.70 \pm 1.38 \times 10^{-10}$
Ad11-FK	9.27×10^{5}	3.27×10^{-4}	5.41×10^{-3}	1.60×10^{-4}	$2.46 \pm 1.50 \times 10^{-11}$
Ad35-FK	3.08×10^{6}	4.66×10^{-4}	1.25×10^{-3}	1.29×10^{-4}	$1.78 \pm 1.04 \times 10^{-11}$

Values are averages of three individual measurements

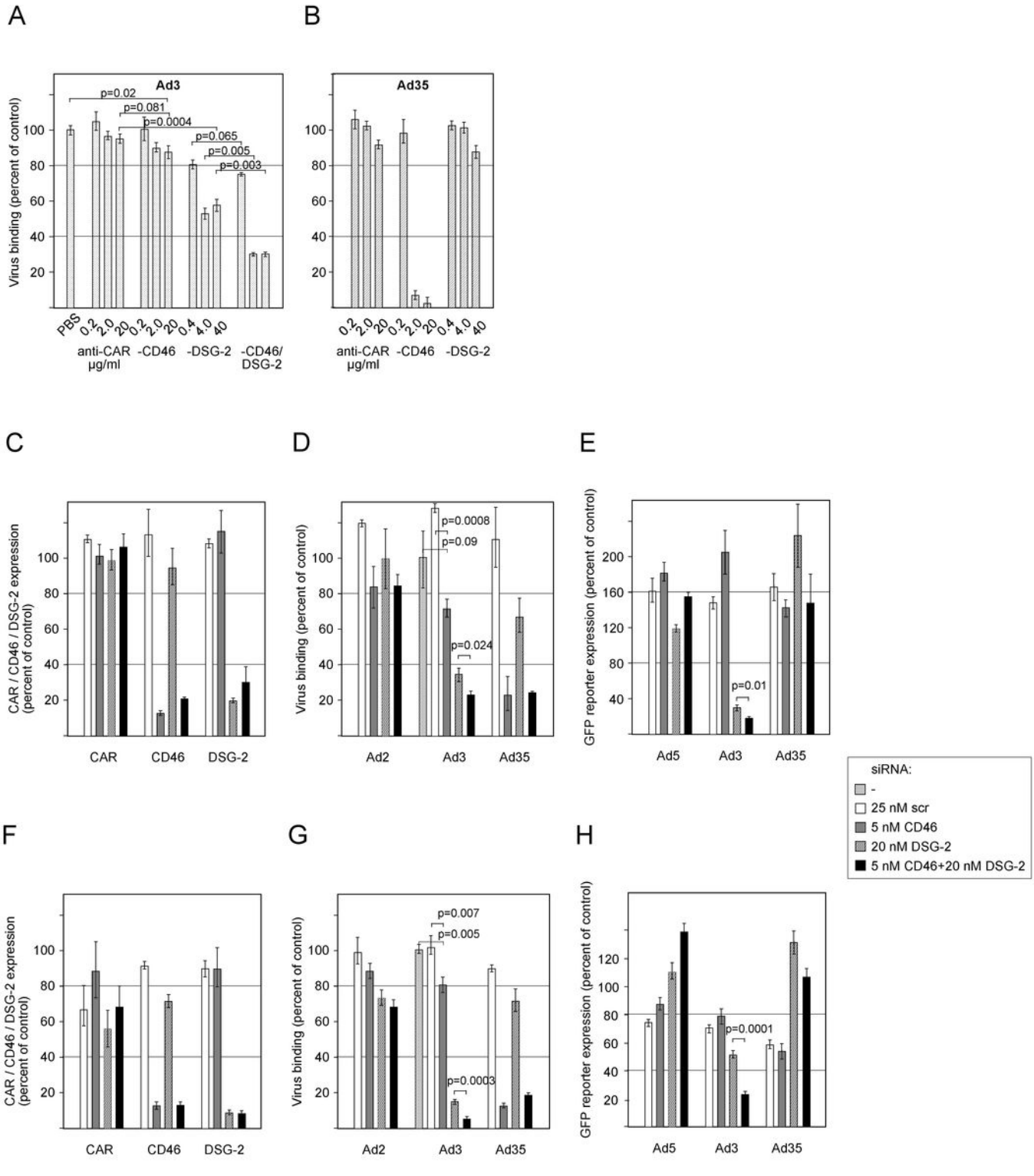

Fig. 1. Loss-of-function studies for individual contribution of CD46 and DSG-2 to Ad3 infection. (A, B) Inhibition of Ad3 (A) and Ad35 (B) binding to A549 cells by anti-CD46 and DSG-2 antibodies. A549 cells were incubated with the indicated concentrations of CD46 (MEM258), DSG-2 (6D8 and 8E5), a mix of both types of antibodies, control CAR antibodies or PBS, followed by the addition of atto-488-labeled Ad3 or Ad35 at 4°'a1C. Virus binding was assesed by cytofluorometric analysis. The data were normalized to the amounts of virus bound when using PBS. Mean values and standard deviations of triplicates from one representative experiment are shown. (C-E) Effect of siRNA-mediated down-regulation on virus infection. (C) A549 cells were transfected with the indicated siRNAs resulting in specific down-regulation of CD46 and DSG-2, but not of unrelated CAR. Shown is one representative analysis. (D) Binding of atto488-labeled Ad2 (control), Ad3 and Ad35 to siRNA-transfected cells was assessed as described above. (E) Transduction of siRNA-transfected cells with eGFP expressing control Ad5, Ad3 and Ad35 vectors at 1,000 vp/cell. eGFP expression values were analyzed two days p.i. by flow cytometry and are expressed as mean fluorescence intensity values (MFI).

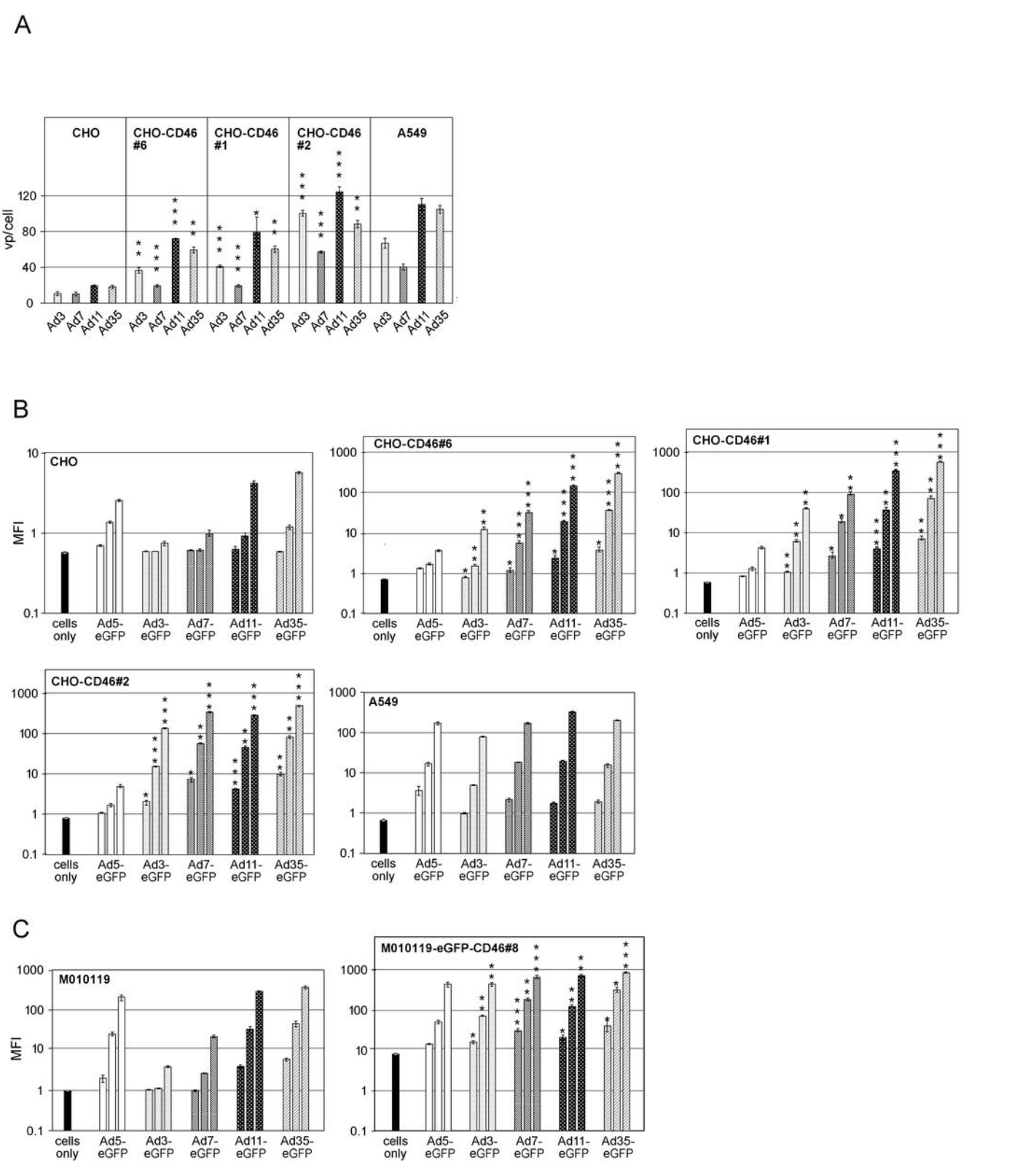

Fig. 2. Binding and transduction of adenovirus species B viruses in CD46 gain-of-function cells negative for DSG-2. (A) For Ad binding assays, 5 x 10^5 of human A549 cells, and the different rodent CHO-CD46 cells were incubated on ice with 1,000 vp of the indicated [^{3}H]-labeled species B serotypes. After incubation for 2 h, the cells were washed and cell-associated radioactivity was determined. Mean values and standard deviations of triplicates from one representative experiment are shown. Asterisks indicate here and in the experiments below the level of significance (*P<0.05; **P<0.005; ***P<0.0005 for comparisons of corresponding Ad binding (infection) in parental CHO versus CD46-transfected cells). (B) Transduction assays of human A549, parental CHO and CHO-CD46 expressing cells. 10^5 cells were incubated with eGFP expressing Ad3, Ad7, Ad11, and Ad35 vectors at increasing virus concentrations of 10, 100, and 1,000 vp/cell. eGFP expression was analyzed two days p.i. by flow cytometry and are expressed as MFI. (C) Transduction assays of human parental and stable CD46-transfected M010119 melanoma cells. Cells were transduced and tested as described above. Background fluorescence intensity for uninfected M010191-eGFP-CD46 cells was higher due to the eGFP-tagged CD46 in these cells.

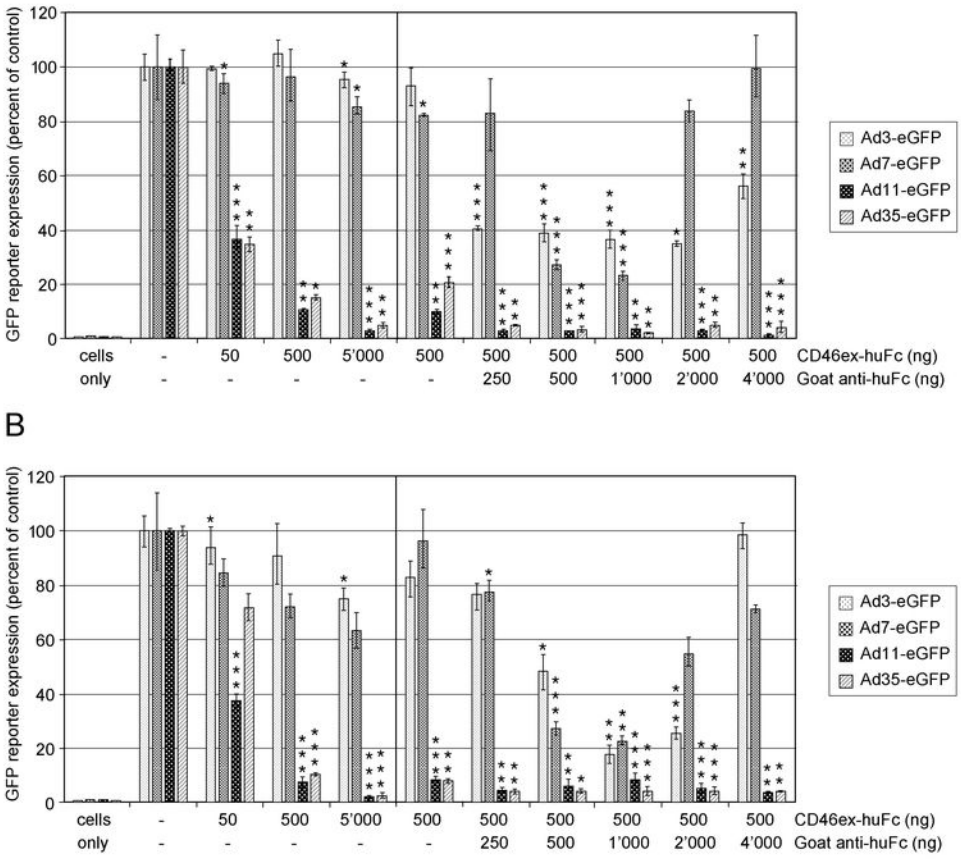

Fig. 3. Cross-linking of CD46ex-huFc strongly increases blocking of Ad3/7 infection in CHO-CD46#2 and A549 cells. (A) CHO-CD46#2 cells or (B) A549 cells were pre-incubated for 1 h in the cold using the indicated concentrations of adapter CD46ex-huFc alone or in combination with a 2-fold increase series of goat-anti human Fc antibody. Following addition of the different eGFP-expressing vectors for another 1 h, cells were washed and analyzed 48 h p.i. Asterisks indicate the level of significance (*P<0.05; **P<0.005; ***P<0.0005 for comparisons of corresponding Ad infection using CD46ex-huFc versus control CARex-huFc of sFig. 2).

A

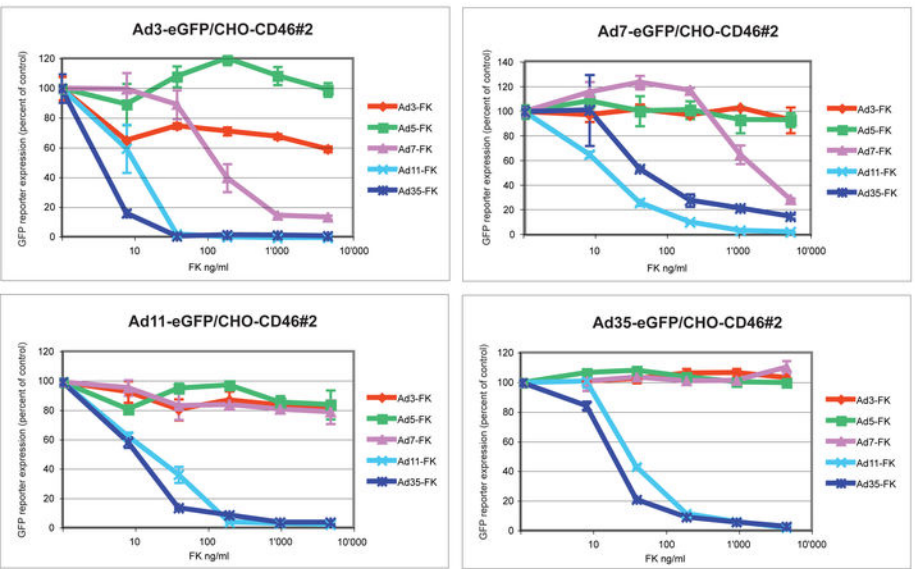

B

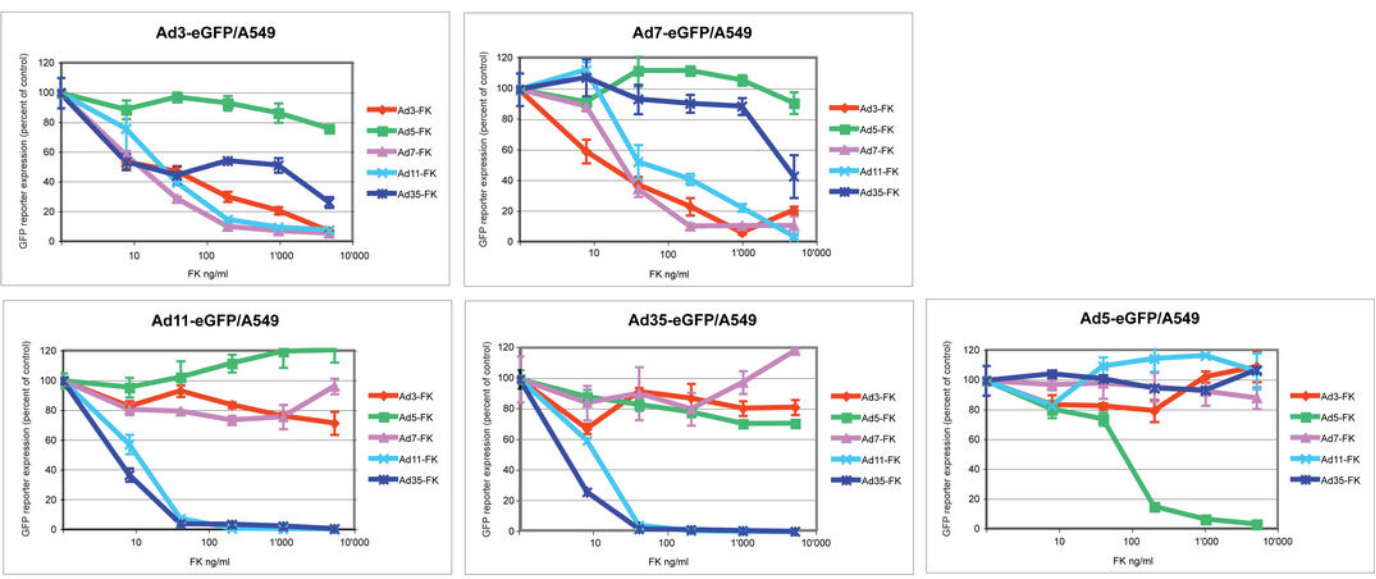

Fig. 4. Inhibition of Ad3-, Ad7-, Ad11-, and Ad35-eGFP transduction in CHO-CD46#2 and A549 cells by recombinant Ad fiber knobs. Cells were pre-incubated for 1 h in the cold using a 5-fold dilution series of the individual FK proteins, followed by addition of the different eGFP-expressing vectors for another 1 h. (A) For CHO-CD46#2 cells, the viral inputs amounted to 29,600, 8,200, 657, and 1,088 vp / cell for Ad3-, Ad7-, Ad11-, and Ad35-eGFP, respectively. The virus input concentrations had been determined in preceding experiments and were chosen such that the unblocked transgene expression values amounted to fluorescence intensity values of about 200. eGFP analysis was performed 48 h p.i.. FKs are colour-coded as follows: Ad5-FK in green, Ad3-FK in red, Ad7-FK in purple, Ad11-FK in cyan and Ad35-FK in dark blue. (B) For A549 cells virus inputs amounted to 14,800, 8,200, 1,314, 2,540 and 2,825 vp/cell for Ad3-, Ad7-, Ad11-, Ad35-, and Ad5-eGFP, respectively. Otherwise, the procedure was the same as above.

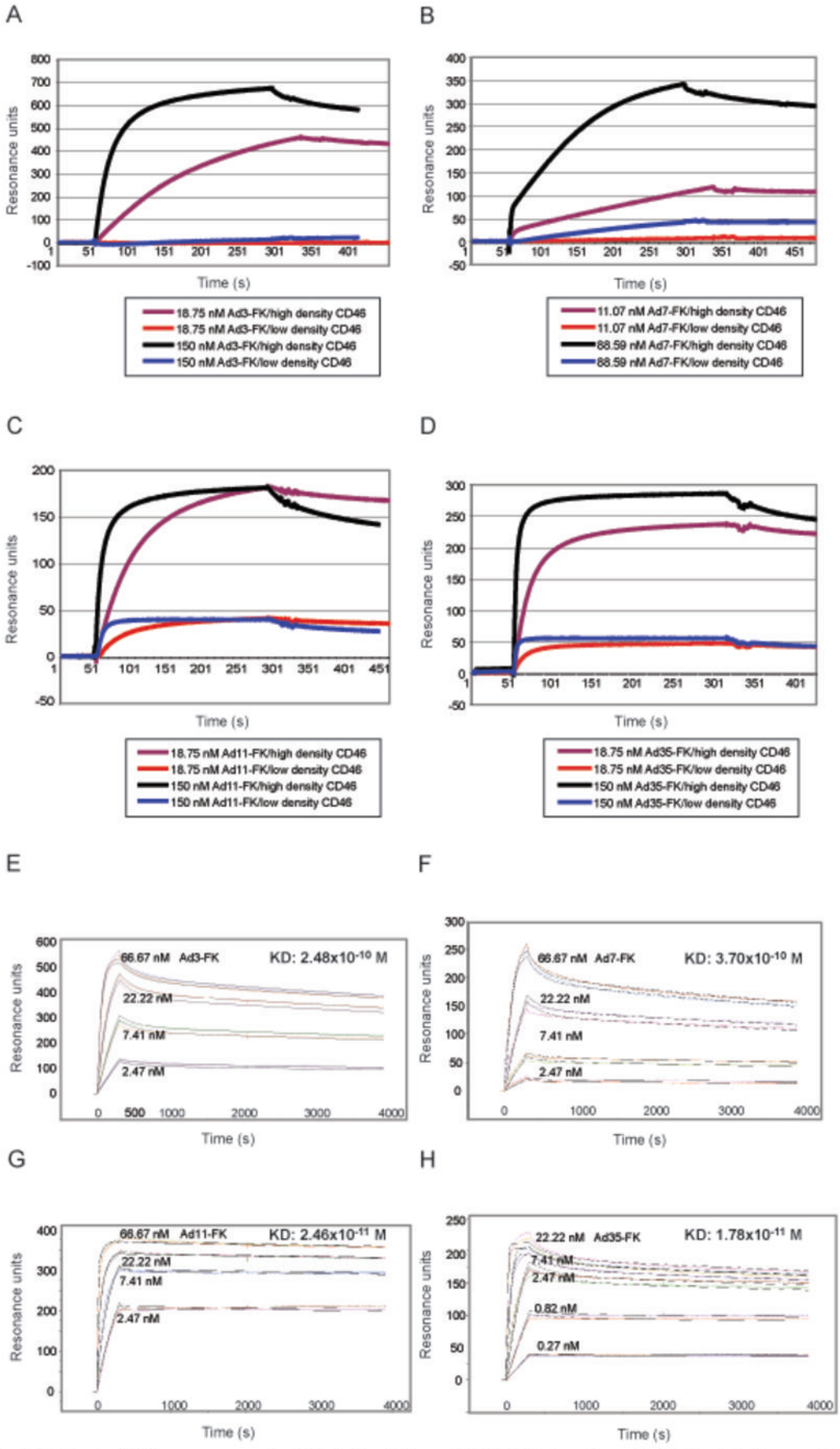

Fig. 5. Subtracted SPR sensograms for Ad3-, Ad7-, Ad11- and Ad35-FK interacting with CD46. Soluble receptor CD46ex-huFc was immobilized on a CM5 chip at high density in Fc2 (2,630 RU) and low density in Fc4 (345 RU). Control CARex-huFc was immobilized at high density in Fc1 (3,431 RU) and low density in Fc3 (278 RU). (A) to (D), FK analytes were injected over the sensor surface at 18.75 and 150 nM concentrations for Ad3-FK (A), Ad11-FK (C) and Ad35-FK (D), and at 11.07 and 88.59 nM for Ad7-FK (B), respectively. Association times were either 240 or 280 s. (E) to (H), overlay of analyte responses for Ad3-, Ad7-, Ad11- and Ad35-FK at different concentrations. Measurements were performed using the CD46 high density 2,630 RU CM5 chip. Serial concentrations of 0.27, 0.82, 2.47, 7.41, 22.22 and 66.67 nM of Ad3-FK (E), Ad7-FK (F), Ad11-FK (G), and Ad35-FK (H) were injected in HBS-P+ buffer at 30 µl/min under contact time of 300 s and dissociation time of 3,600 s (for better visibility only four of the six binding curves are shown). Data evaluation was fitted globally by two-stage reaction model with Biacore T100 evaluation software, and resulting kinetics/affinity results are listed in sTable 1 and summarized in Table 4.

Supplemental Data

Supplemental Methods

Kinetic/affinity analysis and fitting procedure for SPR

Kinetic/affinity analysis of FK binding to immobilized CD46 was performed using three models in combination with the Biacore T100 evaluation software version 2.0.3. A first included a 1:1 fitting model provided by the Biacore T100 evaluation software itself, which failed to describe the obtained binding data satisfyingly. Second, two trivalent models were tested and included the equations described by Lortat-Jacob *et al*. (2) and a variation of the equations described by Fournel *et al*. (1) (Johan Hoebeke, personal communication). Both trivalent models resulted in reasonable good fitting for Ad11- and 35-FK to immobilized CD46 judged by χ^2 values, but they showed relatively large errors for Ad3- and Ad7-FK binding kinetics. Third, a two-stage reaction model was applied to globally fit the binding data, which provided the lowest χ^2 values for all four FK binding reactions. In this model, analyte (A) binds to ligand (B) to form the complex AB, then complex AB changes to ABx, which cannot dissociate directly to A+B. The net reactions are described by equations 1–6, where σ_{kd1}, σ_{kd2}, σ_{ka1}, and σ_{ka2} are standard deviation for individual k_{d1}, k_{d2}, k_{a1}, and k_{a2}, respectively. σKD is the standard deviation for overall K_D.

$$A + B \underset{kd_1}{\overset{ka_1}{\Leftrightarrow}} AB \underset{kd_2}{\overset{ka_2}{\Leftrightarrow}} ABx \quad \text{(Eq.1)}$$

$$A = conc$$

$$B[0] = R\max, \frac{dB}{dt} = -(ka_1 * A * B - kd_1 * AB) \quad \text{(Eq.2)}$$

$$AB[0] = 0, \frac{dAB}{dt} = (ka_1 * A * B - kd_1 * AB) - (ka_2 * AB - kd_2 * ABx) \quad \text{(Eq.3)}$$

$$ABx[0] = 0, \frac{dABx}{dt} = (ka_2 * AB - kd_2 * ABx) \quad \text{(Eq.4)}$$

$$\text{Total response}: AB + ABx + RI$$

$$KD = \frac{kd_1}{ka_1}\frac{kd_2}{kd_2 + ka_2} \quad \text{(Eq.5)}$$

$$\sigma KD = \sqrt{\left(\frac{kd_2}{ka_1(kd_2 + ka_2)}\partial_{ka_1}\right)^2 + \left(\frac{kd_1(kd_2 + ka_2) - kd_1 kd_2}{ka_1(kd_2 + ka_2)^2}\sigma_{kd_2}\right)^2} + \left(\frac{kd_1 kd_2}{ka_1^2(kd_2 + ka_2)}\sigma_{ka_1}\right)^2 + \left(\frac{kd_1 kd_2}{ka_1(kd_2 + ka_2)}\sigma_{ka_2}\right)^2 \quad \text{(Eq.6)}$$

Legends to supplemental figures

SFig. 1. Flow cytometry profiles of CD46 and DSG-2 expression. CD46 was analyzed in A549 human lung cells, parental rodent CHO and three different stable and clonal CHO-CD46 transfectants with increasing CD46 levels (A), in human 16HBE14o bronchial epithelial cells (C), or in parental M010119 and stable transfected M010119-eGFP-CD46#8 cells (E). Numbers after slash indicate MFI values resulting from utilizing the MCI20.6 anti-CD46 antibody (A, C), or GB24 anti-CD46 (stains both, endogenous and eGFP-tagged CD46) (E). Controls using isotype antibody were in the range from 0.8 to 1 (not shown). DSG-2 was analyzed in A549 cells and in parental M010119 cells (B), in 16HBE14o cells (D) and stable transfected M010119-eGFP-CD46#8 cells (F) with 6D8 anti-DSG-2 antibody.

SFig. 2. Control for cross-linking experiment shown in Fig. 3 with CARex-huFc replacing CD46ex-huFc. (A) CHO-CD46#2 cells or (B) A549 cells were pre-incubated for 1 h in the cold using the indicated concentrations of adapter CARex-huFc alone or in combination with a 2-fold increase series of goat-anti human Fc antibody. Following addition of the different eGFP-expressing vectors for another 1 h, cells were washed and analyzed 48 h p.i.

SFig. 3. Analysis of recombinant Ad-FK and CD46ex-huFc proteins. (A, B) Individual FK proteins were produced using the Baculovirus expression system. Purified FK proteins from Ad3, Ad5, Ad7, Ad11, and Ad35 were analyzed by either 12.5% reducing PAGE and sypro ruby red staining (A), or by 10% native PAGE and Coomassie Blue staining (B). (C) Analysis of recombinant CD46ex-huFc. Three µg of purified CD46ex-huFc were analyzed by 10% native PAGE and Coomassie Blue staining.

STable 1. Overview kinetics/affinity analysis of Ad-FKs binding to immobilized CD46ex-huFc

Annalyte / RU chip / binding experiment	Flow rate (ul / min)	k_{a1} ($M^{-1}s^{-1}$) [a]	k_{d1} (s^{-1})	k_{a2} (s^{-1})	k_{d2} (s^{-1})	% χ^2/R_{max}	K_D (M)
Ad3-FK / 1121 / 1	55	2.04×10^{5} (0.0014)	7.11×10^{-4} (0.019)	1.97×10^{-3} (0.0037)	1.64×10^{-4} (0.0022)	0.64 - 1.31	2.68×10^{-10} (0.0093)
Ad3-FK / 1121 / 2	30	1.92×10^{5} (0.0013)	7.18×10^{-4} (0.020)	2.03×10^{-3} (0.0037)	1.65×10^{-4} (0.0022)	0.66 - 1.28	2.81×10^{-10} (0.0101)
Ad3-FK / 2630 / 3	30	2.93×10^{5} (0.0035)	6.36×10^{-4} (0.019)	2.02×10^{-3} (0.0046)	1.98×10^{-4} (0.0029)	1.36 - 2.78	1.94×10^{-10} (0.0079)
Ad7-FK / 1121 / 4	30	4.20×10^{4} (0.012)	3.39×10^{-4} (0.059)	3.77×10^{-3} (0.036)	5.08×10^{-5} (0.061)	0.03 - 0.50	1.07×10^{-10} (0.0249)
Ad7-FK / 2630 / 5	30	2.44×10^{5} (0.0047)	5.88×10^{-4} (0.015)	1.18×10^{-3} (0.0035)	2.58×10^{-4} (0.0064)	0.44 - 0.93	4.32×10^{-10} (0.0195)
Ad7-FK / 2630 / 6	30	1.44×10^{5} (0.0046)	3.30×10^{-4} (0.011)	8.67×10^{-4} (0.048)	2.90×10^{-4} (0.015)	0.25 - 0.71	5.72×10^{-10} (0.0419)
Ad11-FK / 1121 / 7	30	9.04×10^{5} (0.021)	9.86×10^{-5} (0.091)	6.96×10^{-4} (0.11)	7.57×10^{-5} (0.39)	2.86 - 5.05	1.07×10^{-11} (0.0531)
Ad11-FK / 2630 / 8	30	7.96×10^{5} (0.012)	3.93×10^{-4} (0.018)	1.03×10^{-3} (0.0054)	1.28×10^{-4} (0.01)	0.27 - 3.72	5.47×10^{-11} (0.0527)
Ad11-FK / 2630 / 9	30	1.08×10^{6} (0.00086)	4.90×10^{-4} (0.032)	1.45×10^{-2} (0.023)	2.77×10^{-4} (0.046)	3.52 - 4.19	8.48×10^{-12} (0.199)
Ad35-FK / 1121 / 10	30	3.54×10^{6} (0.0088)	2.16×10^{-4} (0.015)	1.12×10^{-3} (0.0081)	1.06×10^{-4} (0.0037)	0.12 - 3.03	5.23×10^{-12} (0.0751)
Ad35-FK / 2630 / 11	30	2.12×10^{6} (0.0034)	7.96×10^{-4} (0.030)	1.33×10^{-3} (0.0042)	1.51×10^{-4} (0.0049)	0.27 - 3.08	3.85×10^{-11} (0.0222)
Ad35-FK / 2630 / 12	30	3.60×10^{6} (0.0057)	3.85×10^{-4} (0.019)	1.30×10^{-3} (0.0061)	1.31×10^{-4} (0.0076)	0.16 - 4.76	9.76×10^{-12} (0.0833)

[a] values in parentheses are errors of the fitting procedure

References

1. **Fournel, S., S. Wieckowski, W. Sun, N. Trouche, H. Dumortier, A. Bianco, O. Chaloin, M. Habib, J. C. Peter, P. Schneider, B. Vray, R. E. Toes, R. Offringa, C. J. Melief, J. Hoebeke, and G. Guichard.** 2005. C3-symmetric peptide scaffolds are functional mimetics of trimeric CD40L. Nat Chem Biol **1:**377-82.
2. **Lortat-Jacob, H., E. Chouin, S. Cusack, and M. J. van Raaij.** 2001. Kinetic analysis of adenovirus fiber binding to its receptor reveals an avidity mechanism for trimeric receptor-ligand interactions. J Biol Chem **276:**9009-15.

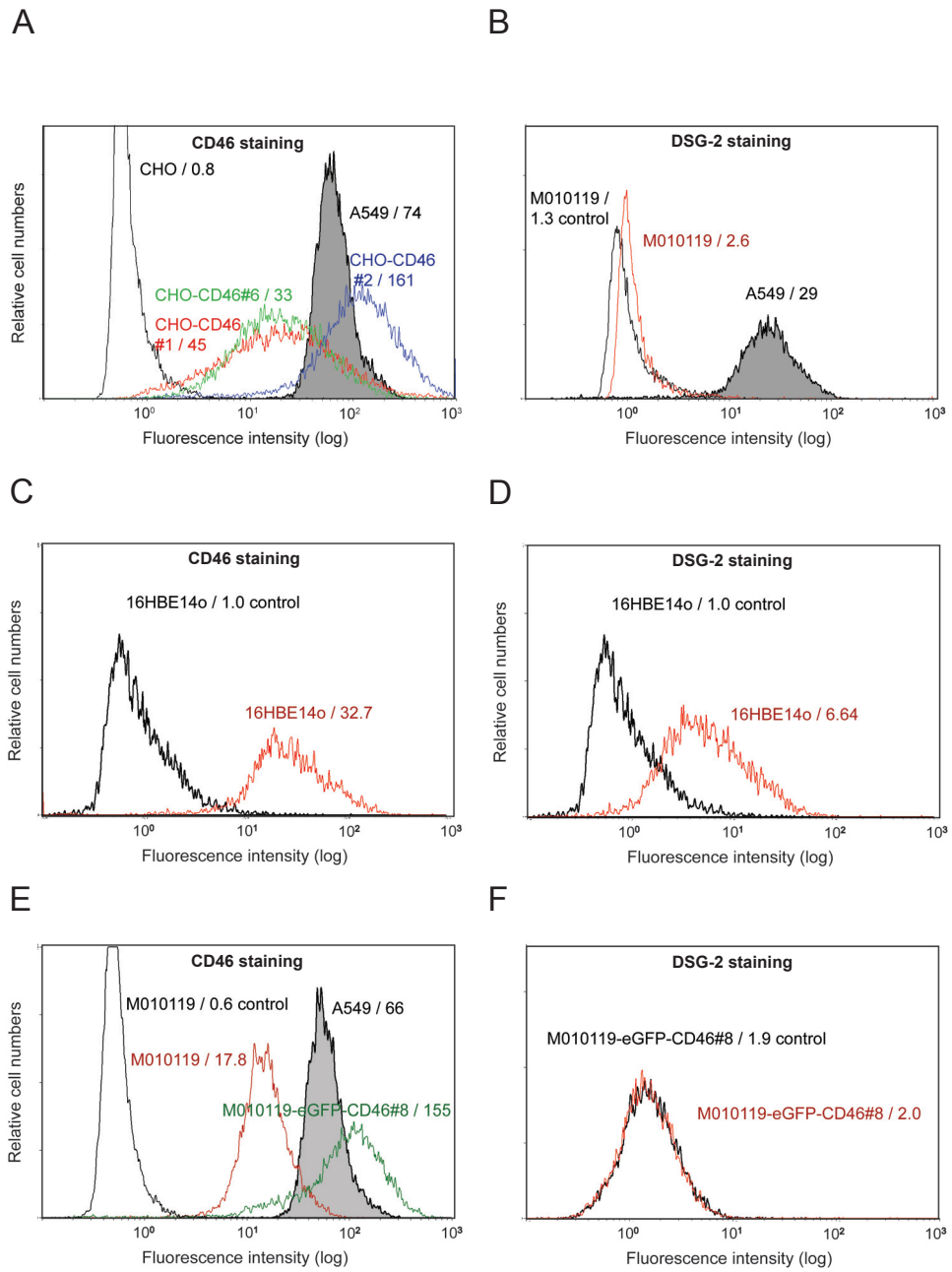

sFig. 1. Flow cytometry profiles of CD46 and DSG-2 expression. CD46 was analyzed in A549 human lung cells, parental rodent CHO and three different stable and clonal CHO-CD46 transfectants with increasing CD46 levels (A), in human 16HBE14o bronchial epithelial cells (C), or in parental M010119 and stable transfected M010119-eGFP-CD46#8 cells (E). Numbers after slash indicate MFI values resulting from utilizing the MCI20.6 anti-CD46 antibody (A), or GB24 anti-CD46 (stains both, endogenous and eGFP-tagged CD46) (E). Controls using isotype antibody were in the range from 0.8 to 1 (not shown). DSG-2 was analyzed in A549 cells and in parental M010119 cells (B), in 16HBE14o cells (D) and stable transfected M010119-eGFP-CD46#8 cells (F) with 6D8 anti-DSG-2 antibody.

A

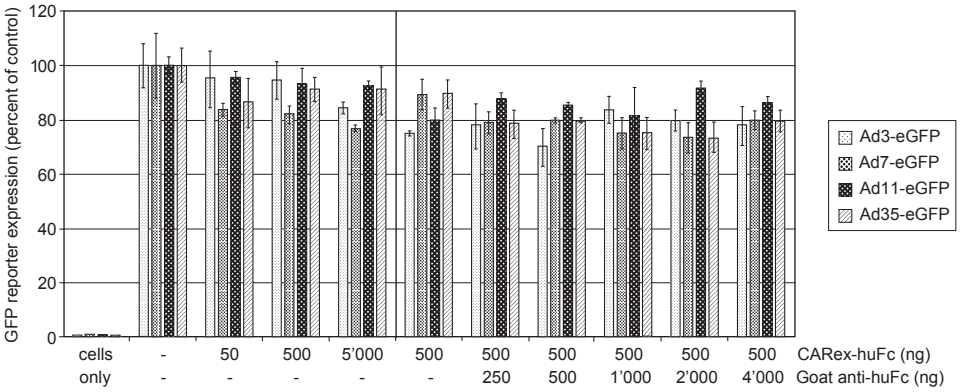

B

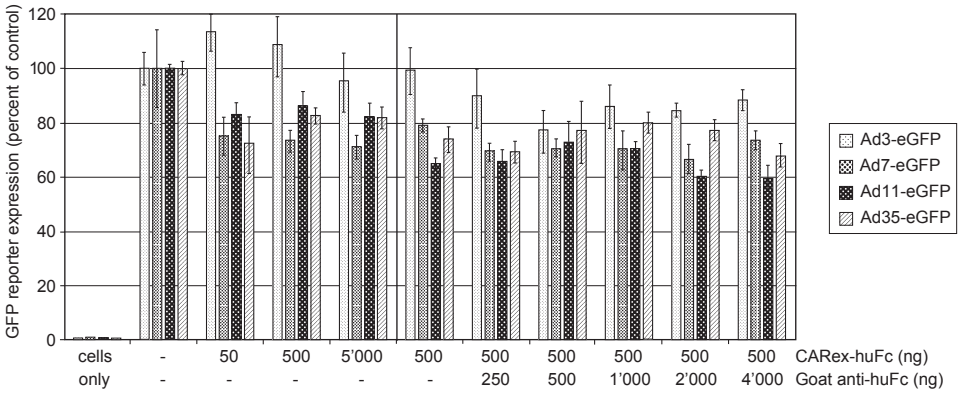

sFig. 2. Control for cross-linking experiment shown in Fig. 3 with CARex-huFc replacing CD46ex-huFc. (A) CHO-CD46#2 cells or (B) A549 cells were pre-incubated for 1 h in the cold using the indicated concentrations of adapter CARex-huFc alone or in combination with a 2-fold increase series of goat-anti human Fc antibody. Following addition of the different eGFP-expressing vectors for another 1 h, cells were washed and analyzed 48 h p.i.

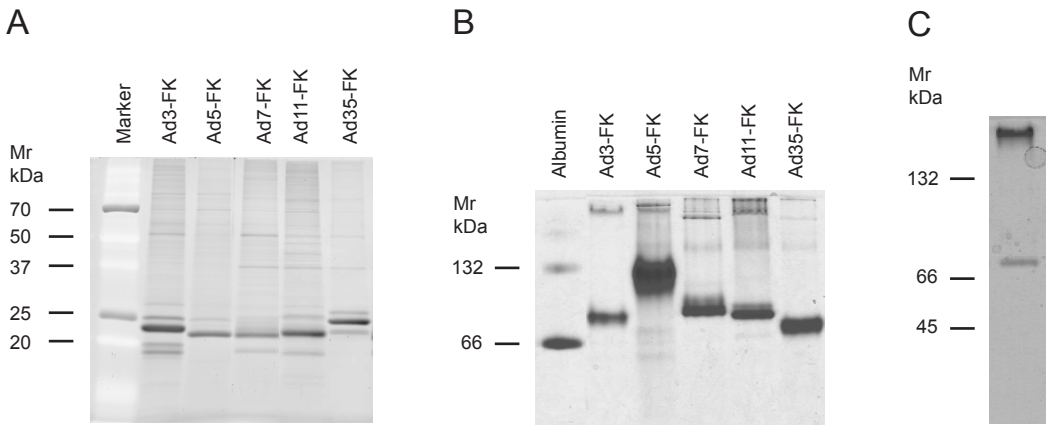

sFig. 3. Analysis of recombinant Ad-FK and CD46ex-Fc proteins. (A, B) Individual FK proteins were produced using the Baculovirus expression system. Purified FK proteins from Ad3, Ad5, Ad7, Ad11, and Ad35 were analyzed by either 12.5% reducing PAGE and sypro ruby red staining (A), or by 10% native PAGE and Coomassie Blue staining (B). (C) Analysis of recombinant CD46ex-huFc. Three µg of purified CD46ex-huFc were analyzed by 10% native PAGE and Coomassie Blue staining.